Supplementary Information

A Small Molecule That Switches a Ubiquitin Ligase From a Processive to a Distributive Enzymatic Mechanism

Stefan G. Kathman[1], Ingrid Span[2], Aaron T. Smith[2], Ziyang Xu[1], Jennifer Zhan[1], Amy C. Rosenzweig[2], & Alexander V. Statsyuk[1*]

[1]Department of Chemistry, and Center for Molecular Innovation and Drug Discovery, Chemistry of Life Processes Institute, Northwestern University, Silverman Hall, 2145 Sheridan Road, Evanston, Illinois 60208

[2]Departments of Molecular Biosciences and of Chemistry, Northwestern University, 2205 Tech Drive, Evanston, Illinois 60208

***e-mail: a-statsyuk@northwestern.edu**

Table of Contents

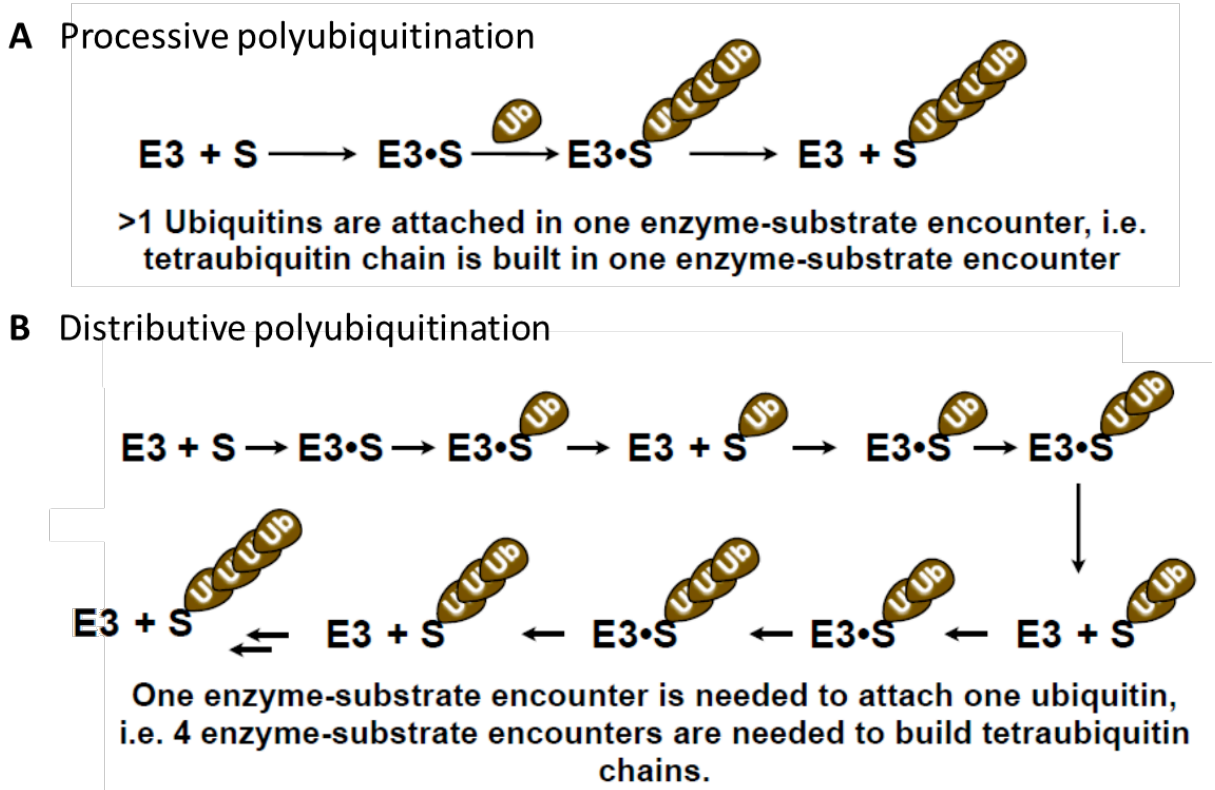

Figure S1. E3 ligases can build polyubiquitin chains with either a processive (A) or distributive (B) enzymatic mechanism. E3: E3 ubiquitin ligase; S: substrate, Ub: ubiquitin.

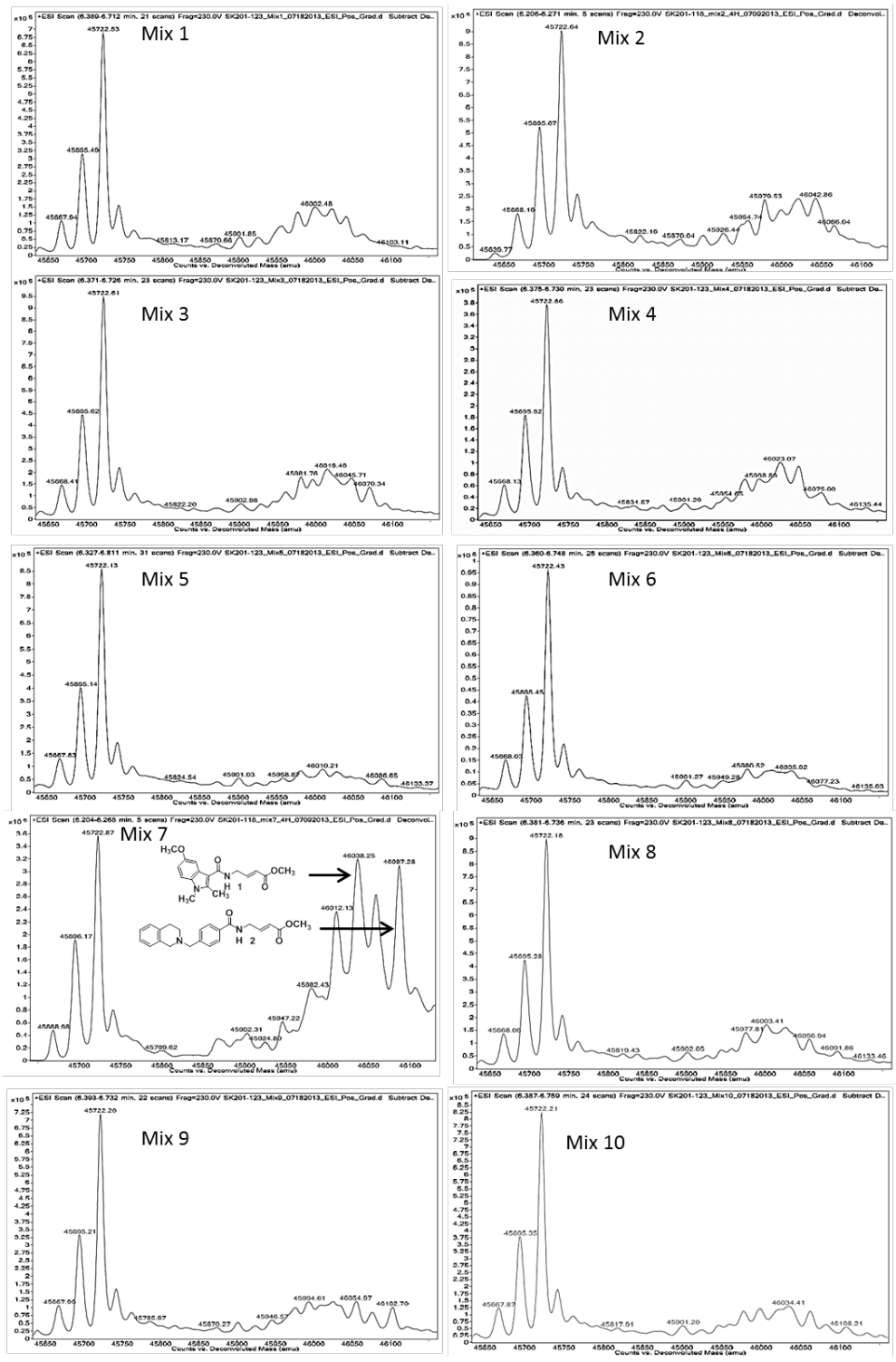

Figure S2. Mass spectrometry (MS) based screening of Nedd4-1 HECT domain and fragments. Mixtures of fragments are the same as reported previously (Ref. 14 of the main manuscript). Mixtures of ten fragments (100 µM each) were incubated with Nedd4-1 HECT domain for 4 h, followed by Zeba column gel filtration and whole protein electrospray ionization MS (ESI-MS). Hits **1** and **2** are shown in mix 7.

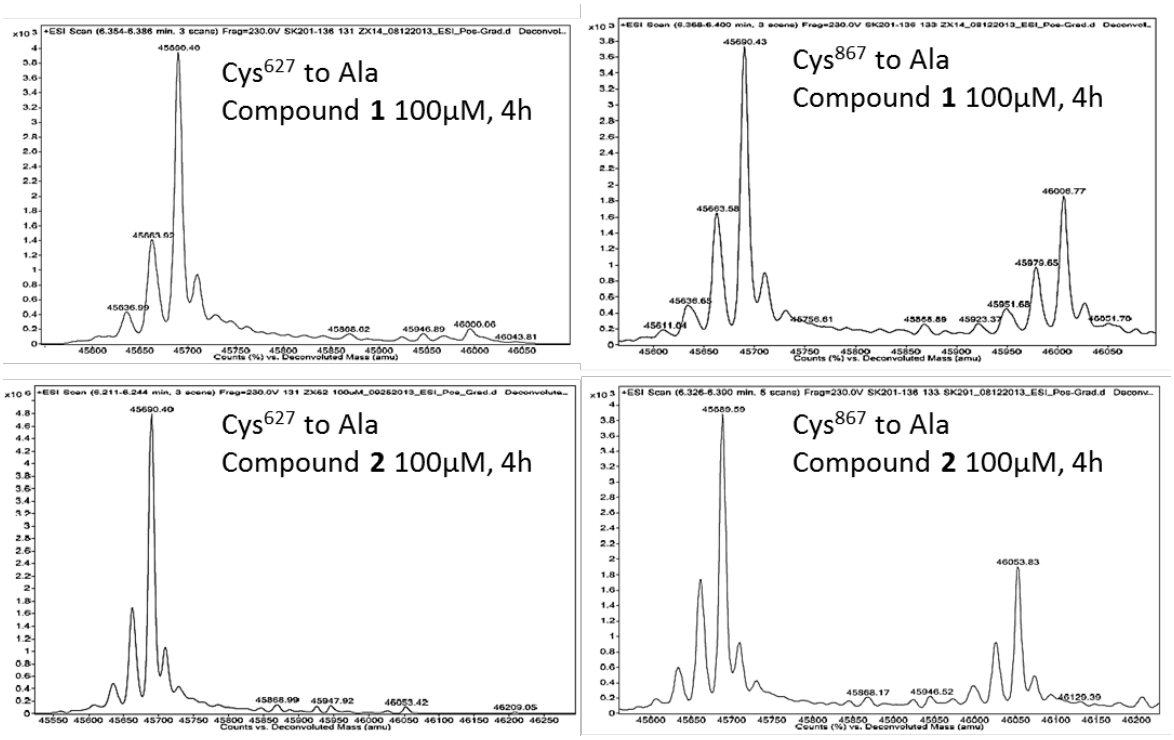

Figure S3. Compounds **1** and **2** selectively modify the non-catalytic Cys^{627} of Nedd4-1. Cys^{627}Ala mutation impairs labeling by compounds **1** and **2**, while the Cys^{867}Ala mutation has no effect. Compounds **1** or **2** at 100 µM in 1% DMSO were incubated with the indicated Nedd4-1 HECT domain mutant (10 µM) for 4 h, followed by Zeba column gel filtration and whole protein ESI-MS.

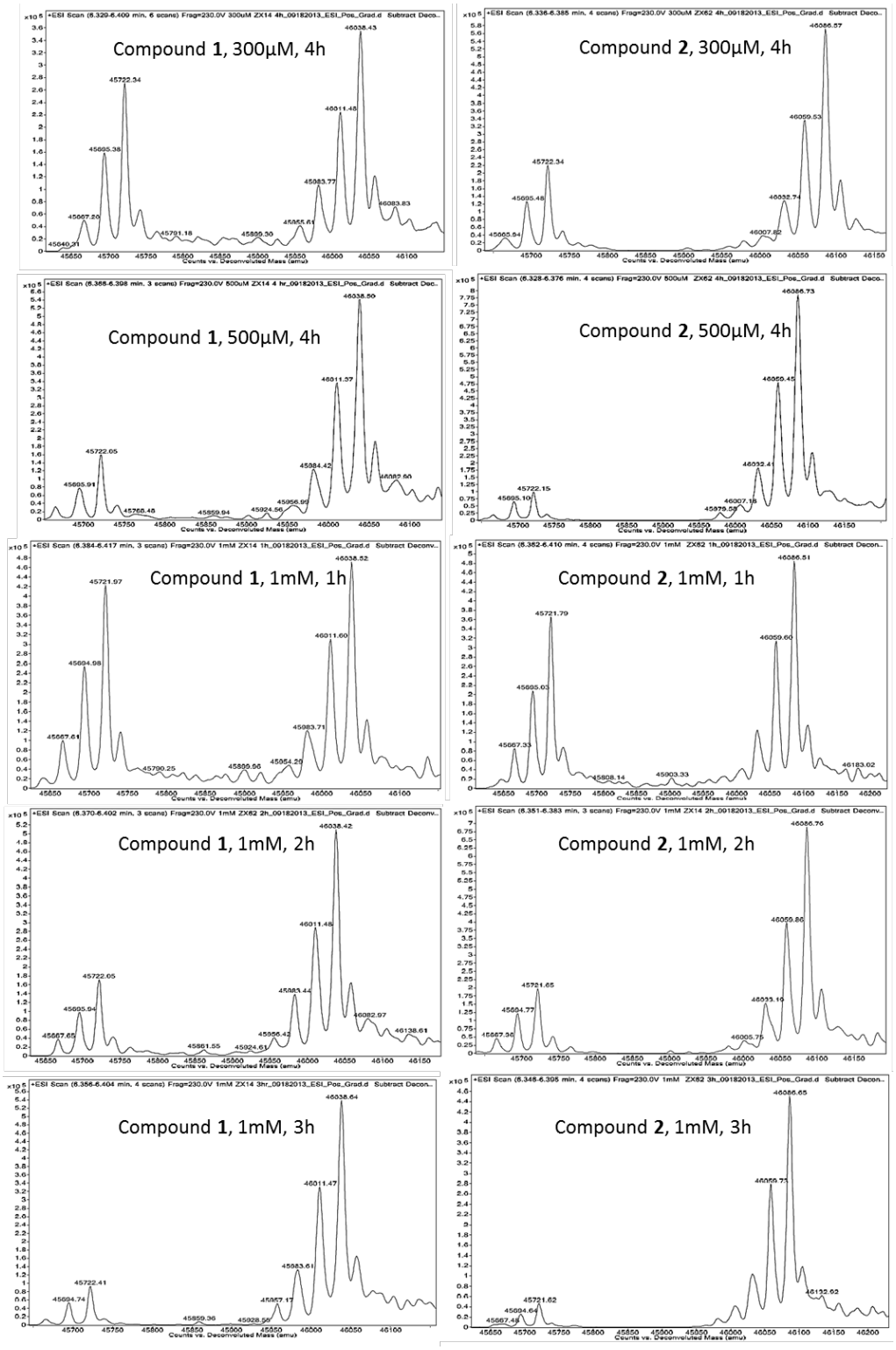

Figure S4. Time- and concentration-dependent covalent modification of Nedd4-1 with compounds **1** and **2**. Compounds **1** or **2** at the indicated concentration in 1% DMSO were incubated with Nedd4-1 HECT domain mutant (10 µM) for the indicated time period, followed by Zeba column gel filtration and whole protein ESI-MS.

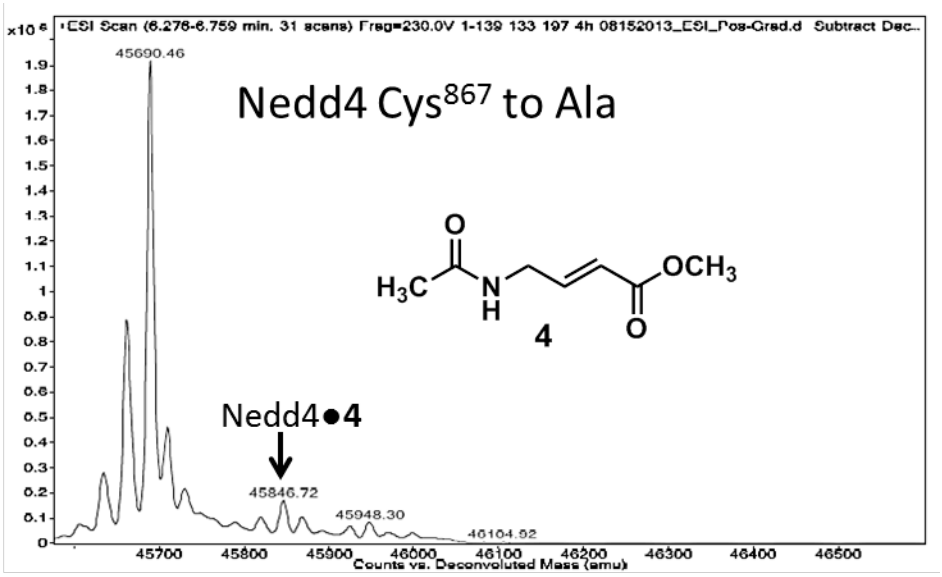

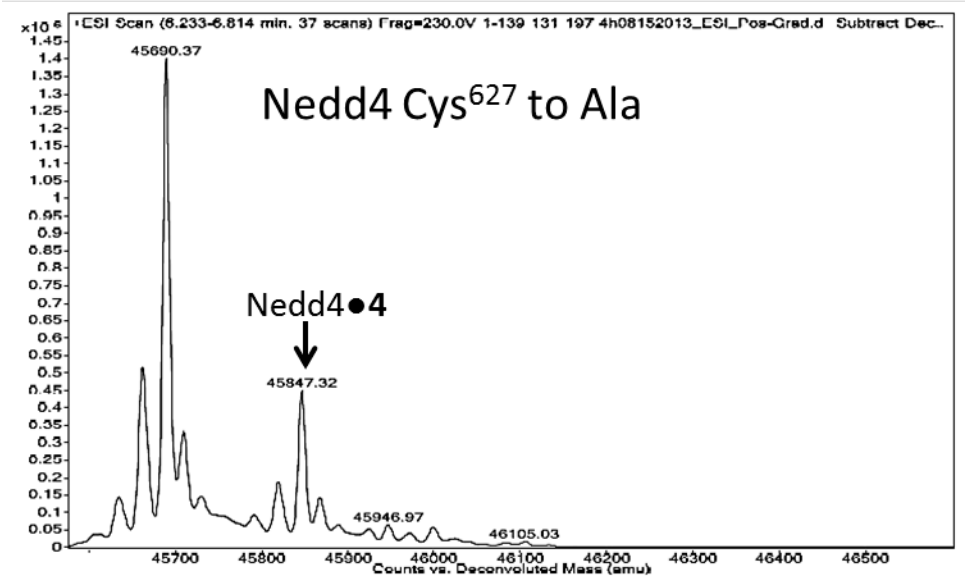

Figure S5. The catalytic Cys^{867} of Nedd4-1 is more reactive with the non-specific N-acetyl electrophile **4** than Cys^{627}, as determined by the corresponding Cys to Ala mutations. Compound **4** at 1 mM in 1% DMSO was incubated with the indicated Nedd4-1 HECT domain mutant (10 µM) for 4h, followed by Zeba column gel filtration and whole protein ESI-MS. Since compound **4** has no fragment directing group, we reasoned that any difference in reactivity between Cys^{867} and Cys^{627} with **4** would be due to an inherent difference in the reactivity of the cysteines with the electrophile itself. Therefore, Cys^{867} is more reactive than Cys^{627}, and without the fragment directing groups our hits would otherwise react with Cys^{867}.

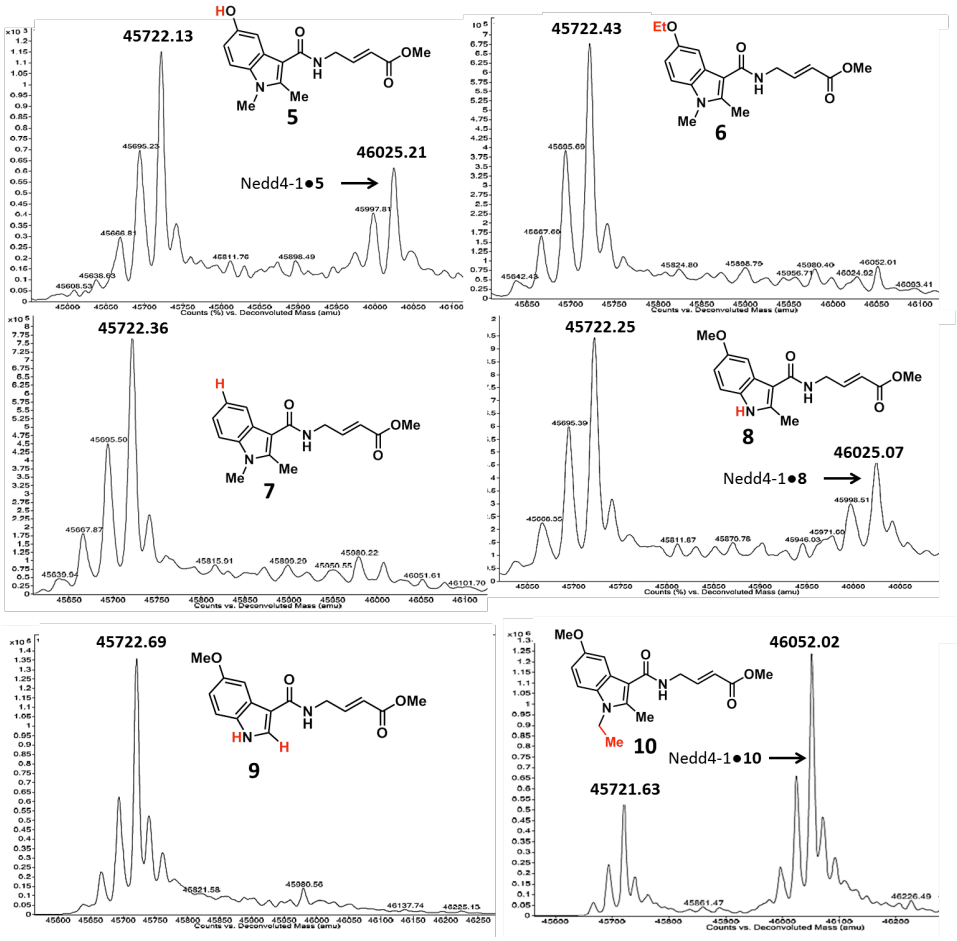

Figure S6. Structural changes in **1** impact covalent labeling of Nedd4-1 HECT domain. Nedd4-1 HECT domain (10 µM) was treated with the indicated compounds at 100 µM for 4 h, followed by Zeba column gel filtration and whole protein ESI-MS. Notably, the 5-position of the indole does not tolerate a 5-CH_3-CH_2-O- substitution, while labeling is improved when N-CH_3 is replaced by N-CH_2-CH_3.

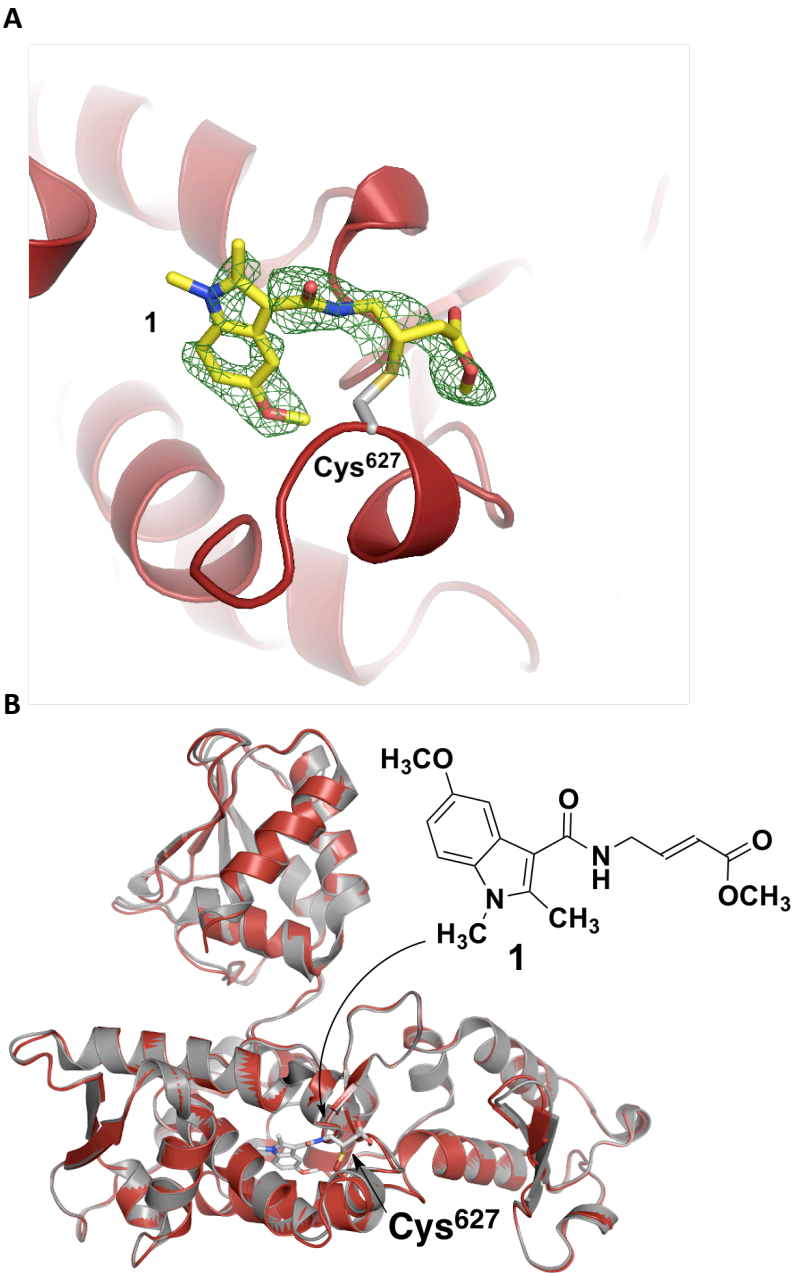

Figure S7. A) Inhibitor-binding site with the side chain of Cys^{627} and **1** depicted as sticks and colored by atom type. The $2F_O - F_C$ electron density map (green mesh, contoured at 1.0 σ) was computed after simulated annealing with the inhibitor omitted from the atomic model. The observation of positive difference density in the simulated annealing omit map clearly indicates the presence of the covalent inhibitor. In the final, refined structure (Fig. 2D, main text), the $2F_O - F_C$ electron density map displays electron density that unambiguously matches **1**. B) Superposition of Nedd4-1 (PDB ID 2XBF) and the Nedd4-1:**1** complex with the protein depicted as a cartoon and the inhibitor as well as the side chain of Cys^{627} shown as sticks.

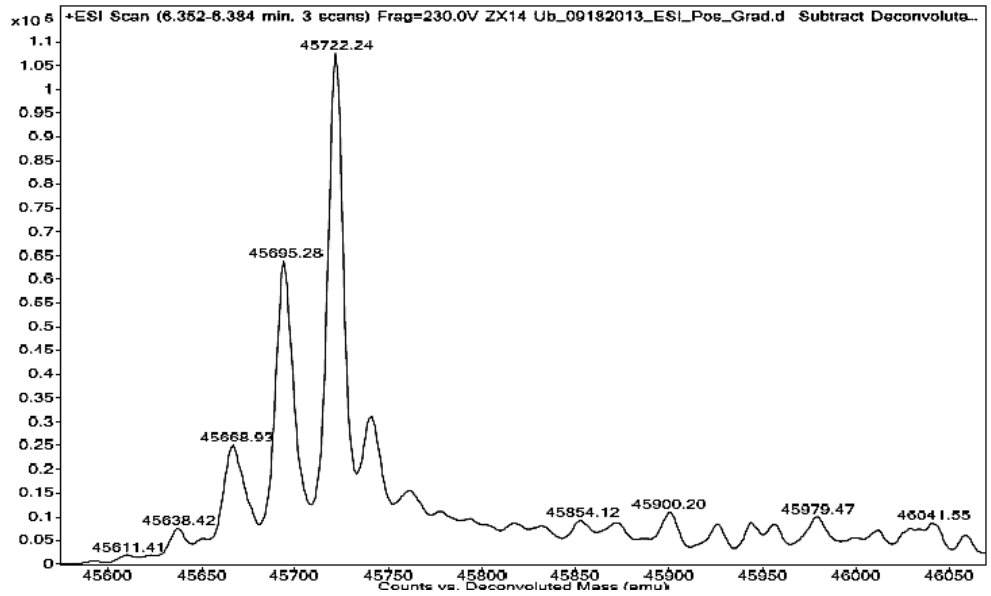

Figure S8. Inhibition of Nedd4-1 labeling with compound **1** in the presence of 60 μM ubiquitin. Compound **1** (100μM) in 1% DMSO was incubated with Nedd4-1 HECT domain (10 μM) and ubiquitin (60 μM) for 4 h, followed by Zeba column gel filtration and whole protein ESI-MS.

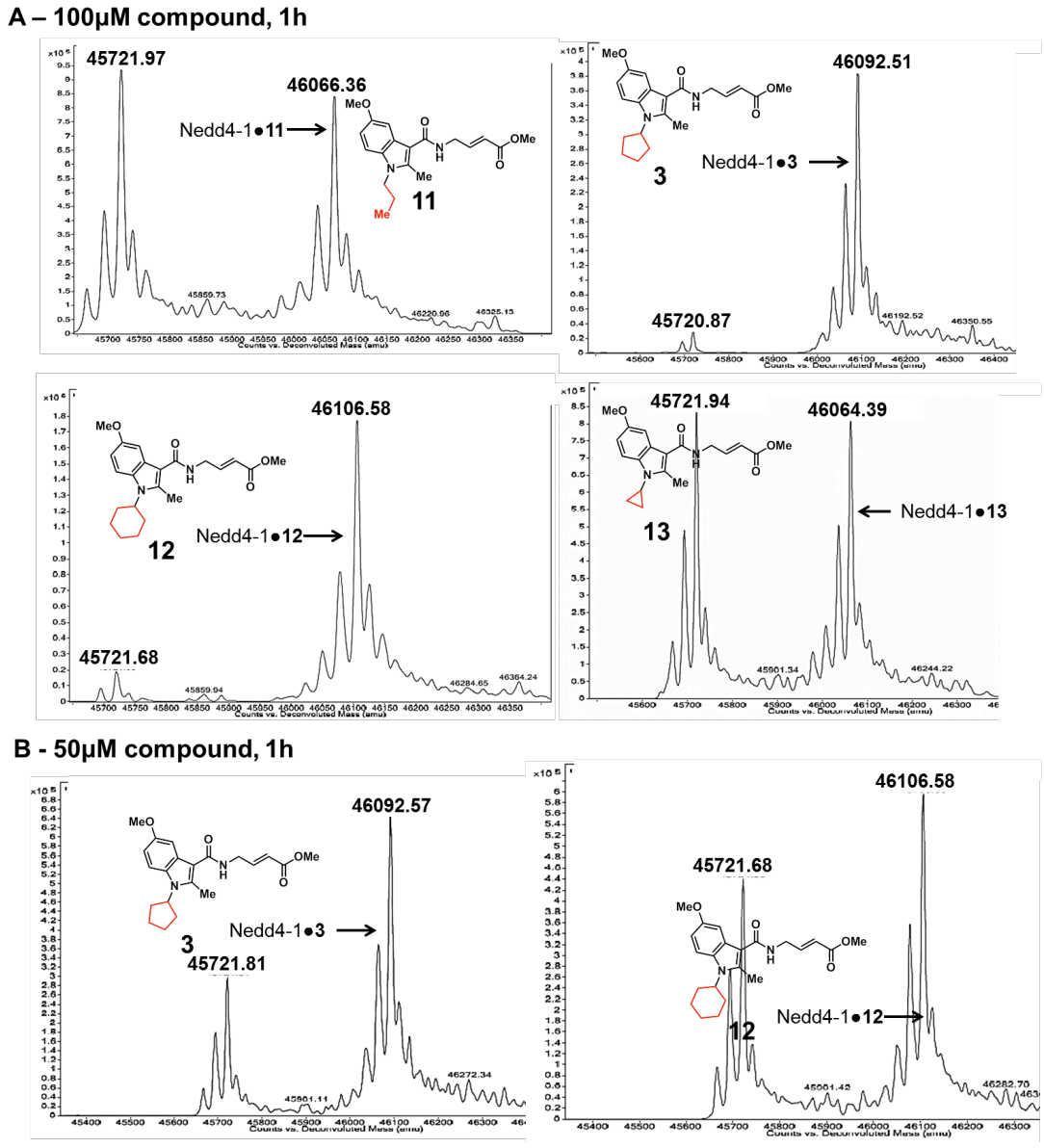

Figure S9. A) Structure activity relationship (SAR) studies of N-substituted indole analogs **3,11-13** designed to improve the potency of compound **1**. Nedd4-1 HECT domain (10 μM) was treated with the indicated compounds in 1% DMSO at 100 μM for 1 h, followed by Zeba column gel filtration and whole protein ESI-MS. B) Studies with 50 μM inhibitor show that **3** is slightly more potent than **12**. Nedd4-1 HECT domain (10 μM) was treated with the indicated compounds in 1% DMSO at 50 μM for 1 h, followed by Zeba column gel filtration and whole protein ESI-MS.

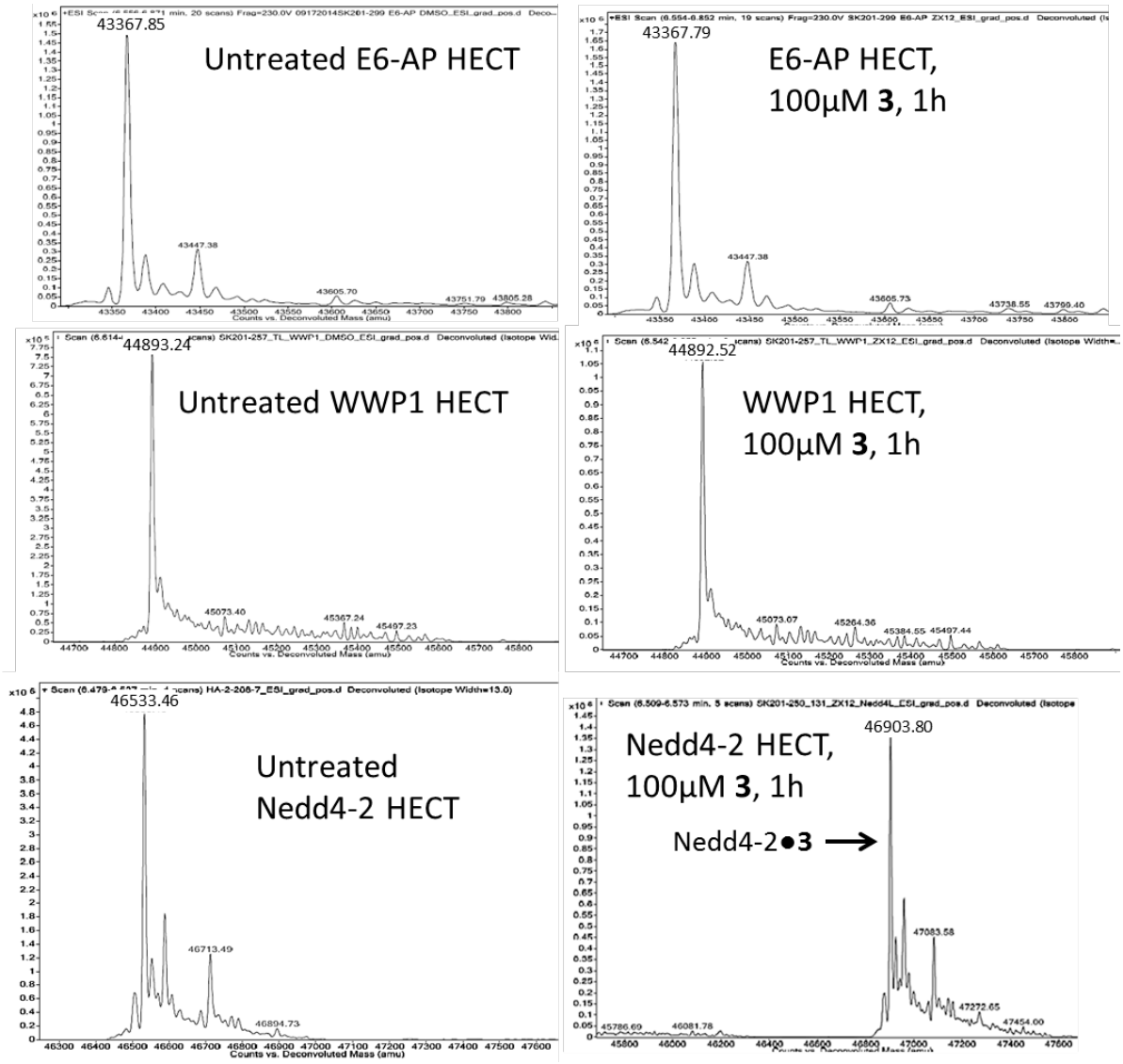

Figure S10. Counterscreen of compound **3** against catalytic HECT domains of E6-AP, WWP1, and Nedd4-2. Compound **3** at 100 µM in 1% DMSO was incubated with the catalytic domain of the indicated HECT E3 (10 µM) for 1 h, followed by Zeba column gel filtration and whole protein ESI-MS.

A

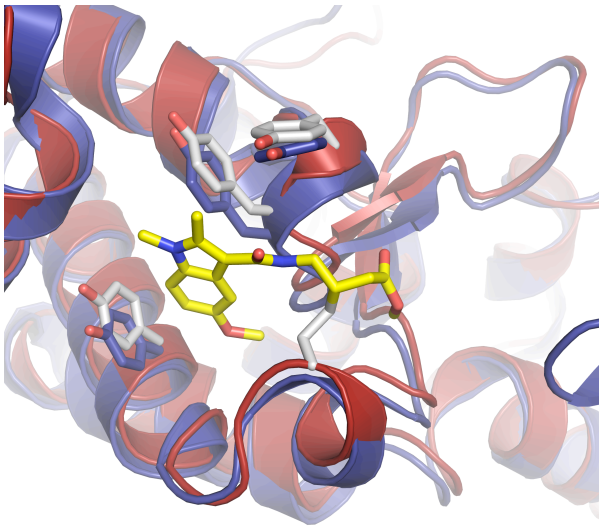

B

```
752 LLLLKELLNP------IYGMFTYYQDSNLLWFSDTCFVEH-------------------- 785 Q15034 HERC3_HUMAN
759 LLIMRELLDP------KYGMFRYYEDSRLIWFSDKTFEDS-------------------- 792 Q5GLZ8 HERC4_HUMAN
731 YCLFAEMIQP------EYGMFMYPEGASCMWFPVKPKFEK-------------------- 764 Q9UII4 HERC5_HUMAN
722 HCMFEEMTKP------EYGMFMYPEMGSCMWFPAKPKPEK-------------------- 755 Q8IVU3 HERC6_HUMAN
1013FLISKEMFNP------YYGLFEYSATDNYTLQINPNSGLCN------------------ 1047P46934 NEDD4_HUMAN
669 FLLSKEMFNP------YYGLFEYSATDNYTLQINPNSGLCN------------------ 703 Q96PU5 NED4L_HUMAN
505 FLLSHEMFNP------FYCLFEYSAYDNYTIQINPNSGIN-------------------- 538 P39940 RSP5_YEAST
617 FLLSHEVLNP------MYCLFEYAGKNNYCLQINPASTIN-------------------- 650 Q9H0M0 WWP1_HUMAN
598 FLLSHEVLNP------MYCLFEYAGKDNYCLQINPASYIN-------------------- 631 Q96J02 ITCH_HUMAN
565 FLLSHEVLNP------MYCLFEYAGKNNYCLQINPASSIN-------------------- 598 O00308 WWP2_HUMAN
449 YLLCHEMLNP------YYGLFQYSTDNIYMLQINPDSSIN-------------------- 482 Q9HCE7 SMUF1_HUMAN
443 YLLSHEMLNP------YYGLFQYSRDDIYTLQINPDSAVN-------------------- 476 Q9HAU4 SMUF2_HUMAN
1301FLLSQELFNP------YYGLFEYSANDTYTVQISPMSAFV-------------------- 1334 Q76N89HECW1_HUMAN
1267FLVSRELFNP------YYGLFEYSANDTYTVQISPMSAFV-------------------- 1300 Q9P2P5HECW2_HUMAN
602 DILSNEIVNP------DYALFTQSADG-TTFQPNSNSYVN-------------------- 634 Q8IYU2 HACE1_HUMAN
4067MIISREMFNP------MYALFRTSPGDRVTYTINPSSHCN-------------------- 4100 Q7Z6Z7HUWE1_HUMAN
576 QLVVEEIFNP------DIGMFTYDESTKLFWFNPSSFETE-------------------- 609 Q05086 UBE3A_HUMAN
466 LLLIRQIFHP------DYGMFTYHKDSHCHWFSSFKCDNY-------------------- 499 Q5U5R9 HECD2_HUMAN
778 NELLKSGFNP------NQGFFKTTNEGLLYPNPAAQMLVG-------------------- 811 Q15386 UBE3C_HUMAN
736 EEIIKRVFDP------ALNLFKTTSGDERLYPSPTSYIHE-------------------- 769 Q7Z3V4 UBE3B_HUMAN
512 ELICKALFDT------TNQLFTRFSDNNQALVHPNPNRPA-------------------- 545 O15033 K0317_HUMAN
1 ------------------------------------------------------------0 Q49AD9 Q49AD9_HUMAN
3656WQVCKELQSS------SLSLLLLCPSSAVNKNKGKYILTPSPIT---------------- 3693 Q9Y4D8K0614_HUMAN
4487AEICEELQNG------LTPLLIVTPNGRDESGANRDCYLLSPAARA-------------- 4526 O95714HERC2_HUMAN
549 ADMSEELCPSSADTPVPLPFFVRTANQGNGTGEARDMYVPNPS----------------- 591 Q5T447 HECD3_HUMAN
4533TEMCQELETG------IVDLLIPSPNATAEVGYNRDRFLFNPSACL-------------- 4572 Q15751HERC1_HUMAN
1636ALVSQELQRADLGLWRGEEVTLSNPKGSQEGTKYIQNLQGLFALPF-----GRTAKPAHI 1690 Q14669TRIPC_HUMAN
2489DMDLDDTDDGD----DNAPLFYQPGKRGFYTPRPGKNTEAR------------------- 2525 O95071UBR5_HUMAN
2179ALVAAEFQRTDLGAWLCDDNFPDDESRHVDLGGGLKPPGYYVQRSCGLFTAPFPQDSDEL 2238 Q9ULT8HECD1_HUMAN
```

Figure S11. A) Superposition of Nedd4-2 (PDB ID 2ONI: blue) and the binding site of **1** in the Nedd4-1:**1** complex (red); the protein is depicted as a cartoon, the inhibitor and the side chains of Cys^{627}, Tyr^{604}, Tyr^{605}, Tyr^{634}, Tyr^{659} (2ONI), Tyr^{660} (2ONI), Tyr^{689} (2ONI) are shown as sticks. B) Sequence alignment of all HECT E3s showing that the cysteine (red) that compound **3** targets is present only in two HECT E3s.

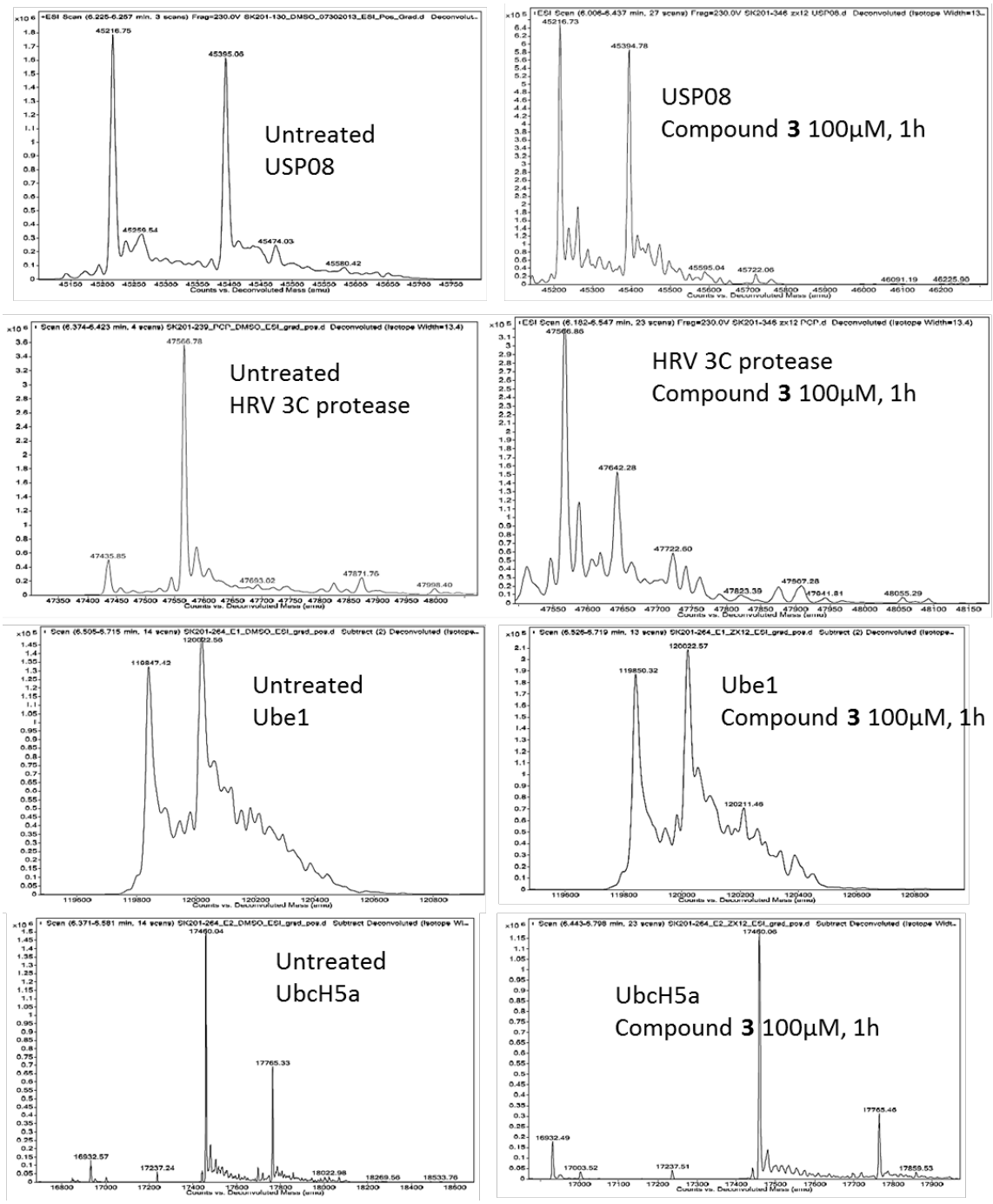

Figure S12. Counterscreen of compound **3** against the deubiquitinase USP08, Human Rhinovirus (HRV) 3C protease, the ubiquitin-activating E1 enzyme Ube1, and the ubiquitin-conjugating E2 enzyme UbcH5a, all of which have catalytic cysteines. Compound **3** at 100 µM in 1% DMSO was incubated with the indicated enzyme (10 µM) for 1 h, followed by gel filtration and whole protein ESI-MS.

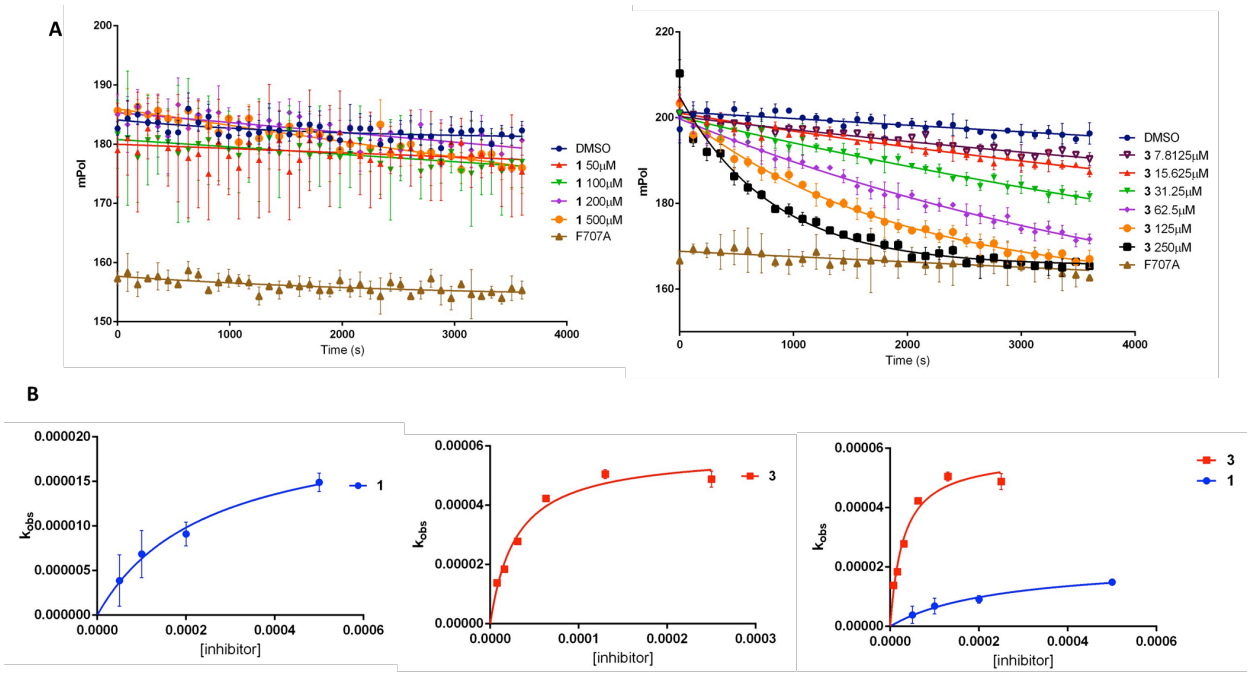

	k_{inact}	K_I	k_{inact}/K_I
1	2.2 ±.232x10^{-5} s^{-1}	245.8±54.8 μM	.089±.029 M^{-1}s^{-1}
3	5.8 ±.358x10^{-5} s^{-1}	29.3±5.91 μM	1.98±.52 M^{-1}s^{-1}

Figure S13. A) Potency of inhibitors **1** and **3** at disrupting Nedd4-1:Ub interactions as assessed by fluorescence polarization. Nedd4-1 HECT and ubiquitin-fluorescein were treated with the indicated concentration of inhibitor in 1% DMSO. Changes in fluorescence polarization were monitored over 1 h. All reactions were performed in triplicate and plotted as mean ± s.e.m. B) k_{obs} vs [inhibitor] plots showing a two step mechanism for the covalent modification of Nedd4-1, in which the initial non-covalent Nedd4-1:inhibitor complex is formed, followed by the covalent bond formation step. k_{obs} values were determined from the slopes of the log plots of (A). Compound **3** is 22.2-fold more potent than compound **1**. All reactions were performed in triplicate and plotted as mean ± s.e.m.

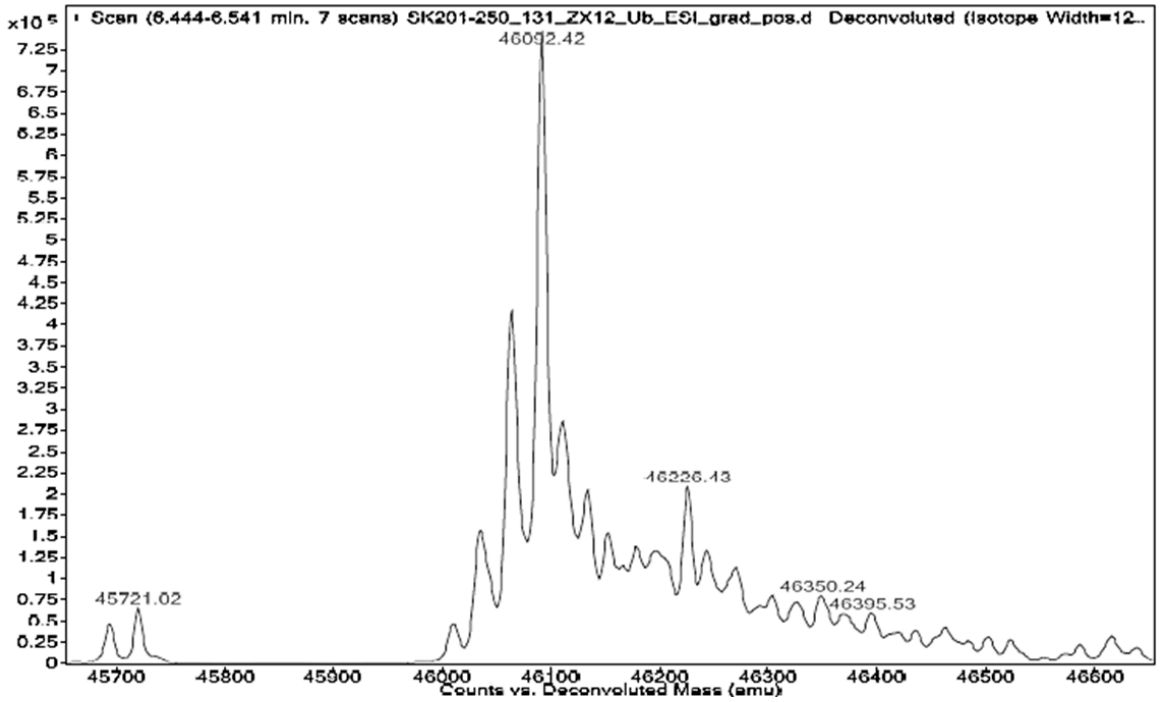

Figure S14. Compound **3** completely labels Nedd4-1 HECT domain in the presence of 60 μM ubiquitin, which is significantly above the Nedd4-1:Ub K_d value of 11 μM. Compound **3** at 100 μM in 1% DMSO was incubated with Nedd4-1 HECT domain (10 μM) and ubiquitin (60 μM) for 4 h, followed by Zeba column gel filtration and whole protein ESI-MS.

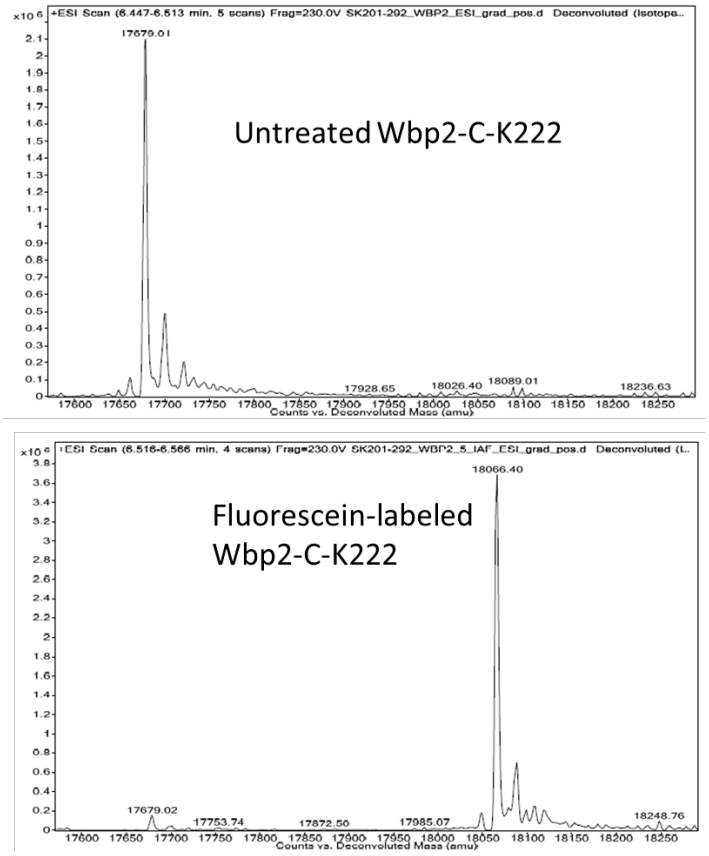

Figure S15. Covalent labeling of Wbp2-C-K222 with 5–iodo-acetamidofluorescein (3 mM, 90 min, 4°C).

Wbp2-C-K222 sequence:

GPLGSSRRAS VGSPEFTMLT FTAGGAIEFG QRMLQVASQA SRGEVPSGAY GYSYMPSGAY VYPPPVANGM YPCPPGYPYP PPPPEFYPGP PMMDGAMGYV QPPPPPYPGP MEPPVSGPDV PSTPAAEAKA AEAAASAYYN PGNPHNVYMP TSQPPPPPYY PPEDRRTQ

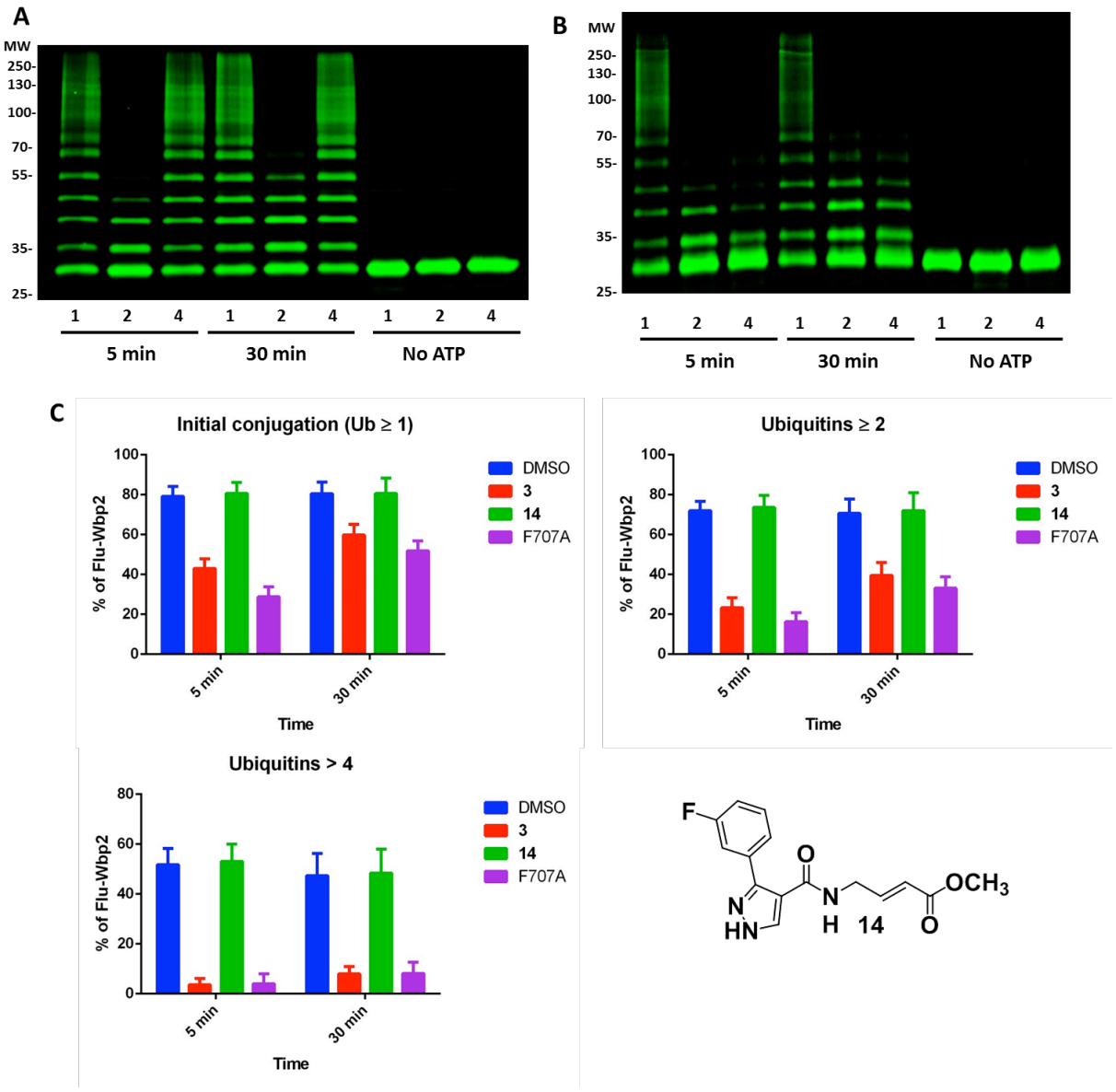

Figure S16. A) Nedd4-1 HECT domain treated with 1% DMSO (lane 1), compound **3** (lane 2), or non-hit electrophile **14** (lane 3) was incubated with E1 and E2 enzymes, ubiquitin, Flu-Wbp2 and ATP. Reaction mixtures were quenched at the indicated times and the amount of ubiquitinated Flu-Wbp2 was determined using in-gel fluorescence. B) Same as in (A) but with the F707A mutant (lane 4) C) Quantification of fluorescent bands from (A) and (B) showing that both initial monoubiquitination and polyubiquitination are disrupted by inhibitor **3**, but polyubiquitination is more greatly affected. This effect is comparable to the Nedd4-1 F707A mutation. Fluorescent Wbp2-C-K222 bands with the indicated number of ubiquitins are plotted as percent of total Wbp2-C-K222 bands (non-ubiquitinated + polyubiquitinated). Reactions were performed in duplicate and presented as mean ± s.e.m. Compound **14** is an electrophilic compound from the original screening library that did not react with Nedd4-1 HECT domain.

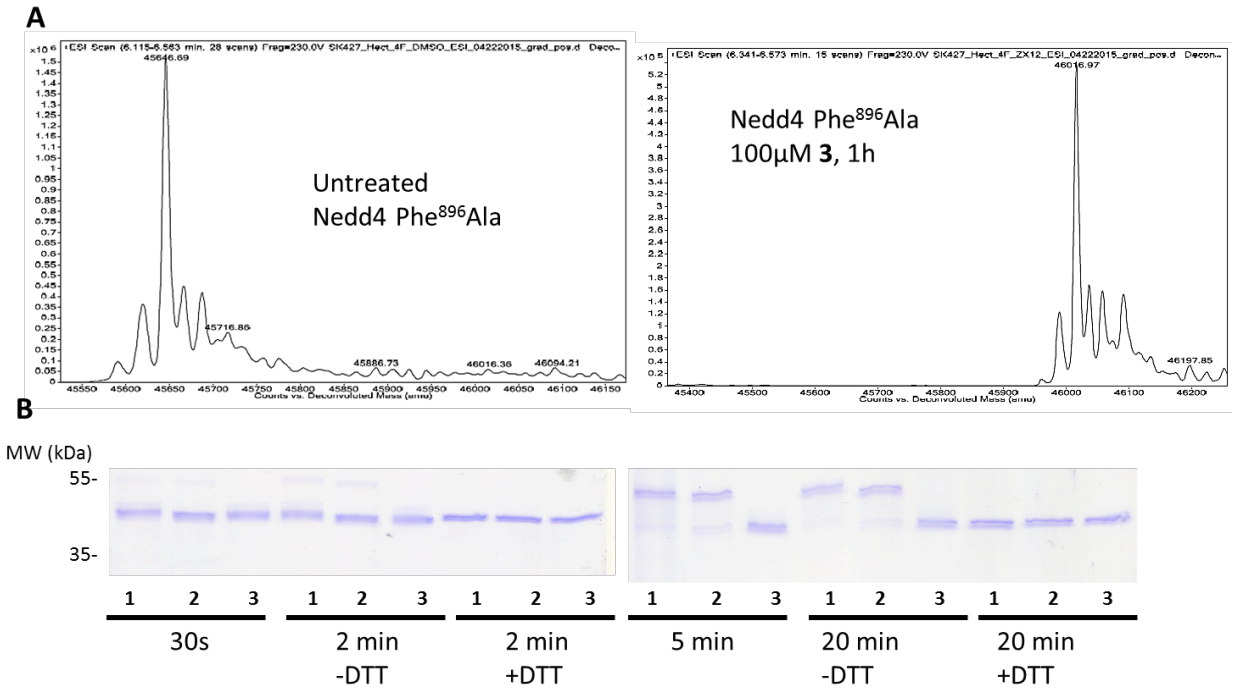

Figure S17. Nedd4-1~Ub thioester formation is unaffected by inhibitor **3**. A) Nedd4-1 HECT Phe^{896}Ala, which can form a Nedd4-1~Ub thioester but cannot discharge Ub was prepared and reacted with compound **3** (100µM, 1h). B) Nedd4-1 HECT Phe^{896}Ala was treated with 1% DMSO (lane 1) or compound **3** (lane 2) without subsequent Zeba column gel filtration, then incubated with E1 and E2 enzymes, ubiquitin, and ATP. Reaction mixtures were quenched with Laemmli buffer (-DTT) at the indicated times and the amount of Nedd4-1~Ub thioester was visualized by Coomassie staining. Lane 3 is a no ATP control reaction. This figure shows that compound **3** does not inhibit E1, E2, or the E2~Ub to E3~Ub transthiolation.

Untreated Nedd4-1 full length E554A

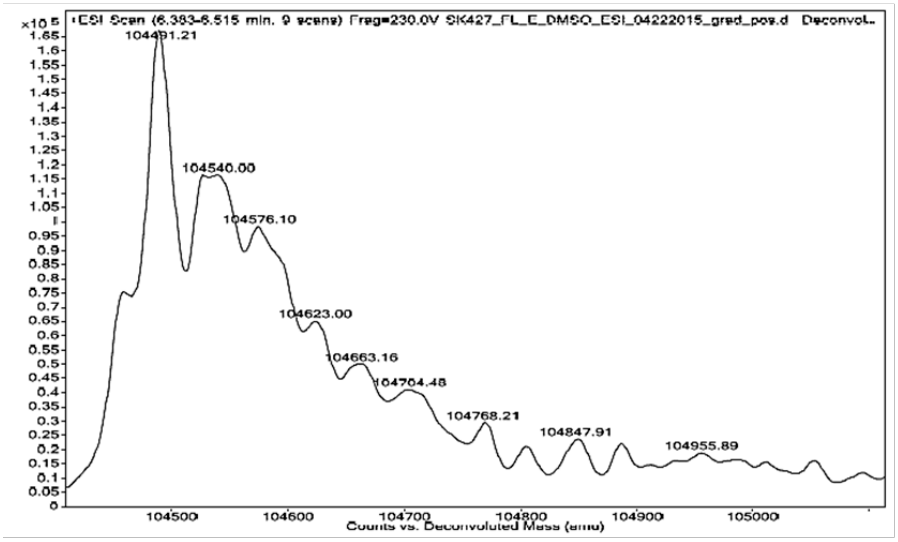

Nedd4-1 full length E554A, 100µM **3**, 1h

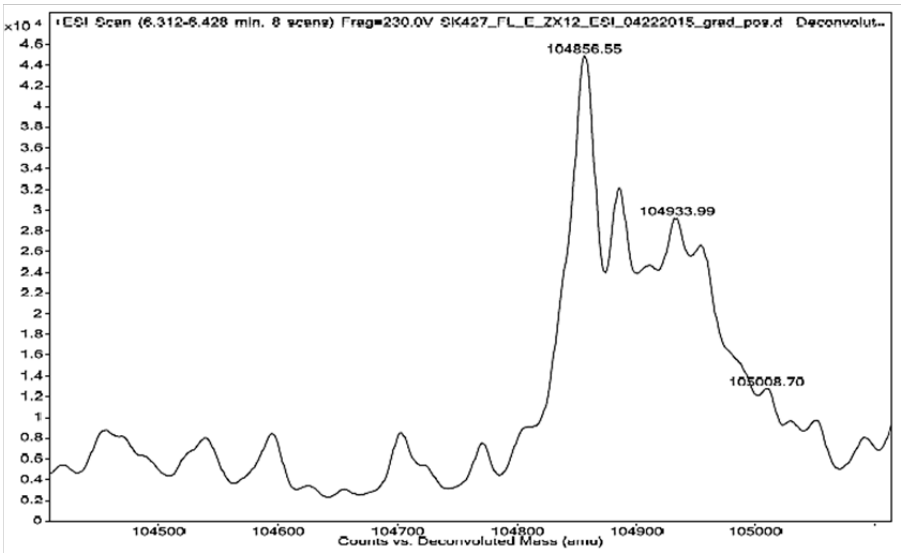

Figure S18. Compound **3** reacts with Nedd4-1 full-length E554A. Compound **3** at 100 µM in 1% DMSO was incubated with Nedd4-1 full-length E554A (10 µM) for 1 h, followed by gel filtration and whole protein ESI-MS.

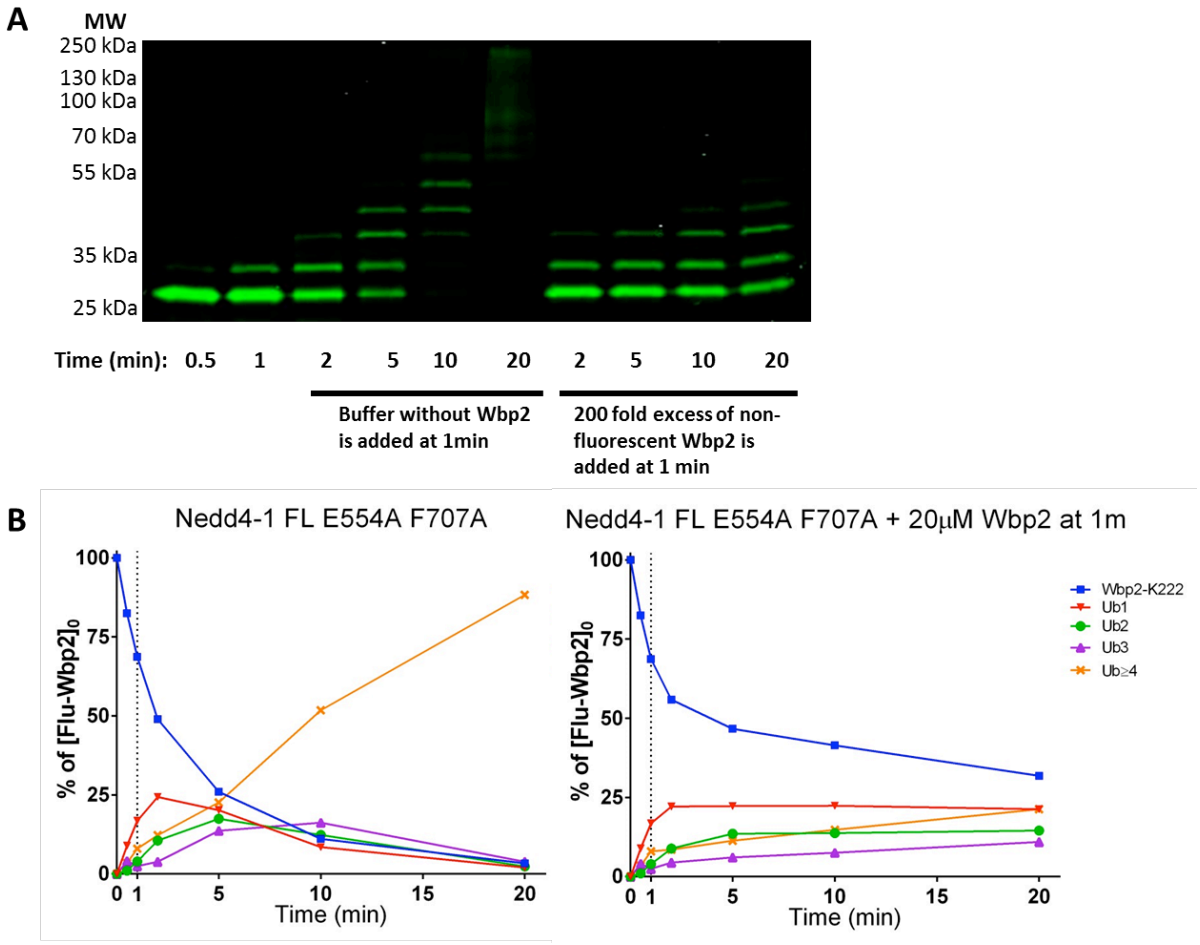

Figure S19. Nedd4-1 full-length E554A F707A is also distributive. Full-length Nedd4-1 E554A F707A (150 nM) was incubated with fluorescent Flu-Wbp2 substrate (100 nM) in the presence of ATP, Ub, E1 and E2 enzymes. After 1 min, a 200-fold excess of non-fluorescent Wbp2 substrate or empty buffer was added to the reaction mixture, and further ubiquitination of Flu-Wbp2 was monitored. B) The amount of ubiquitinated Wbp2 in (A) was plotted as a function of time.

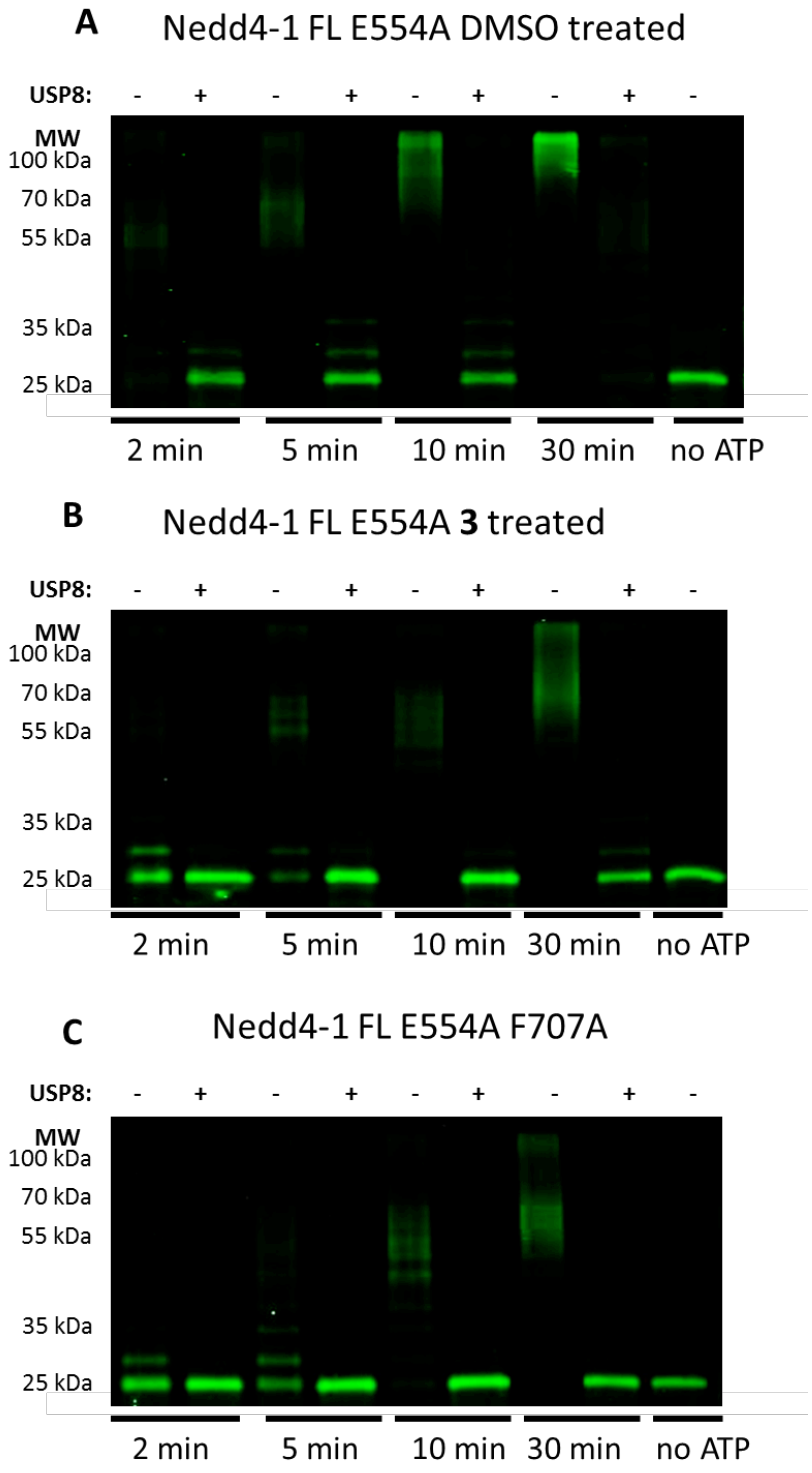

Figure S20. Ubiquitination of Flu-Wbp2 at different time points in the presence or absence of the deubiquitinating enzyme USP8 (200 nM catalytic domain) shows that distributive Nedd4-1 is inhibited by USP8 but processive Nedd4-1 is not. A) DMSO-treated Nedd4-1 full-length E554A; B) compound **3** treated Nedd4-1 full-length E554A; C) Nedd4-1 full-length E554A F707A.

Crystallographic table

	NEDD4-1•compound 1
Data collection	
Space group	*C*2
Cell dimensions	
a, *b*, *c* (Å)	175.20, 38.73, 60.36
α, β, γ (°)	90.00, 93.13, 90.00
Resolution (Å)	32.20 - 2.44 (2.50 – 2.44)
R_{merge} (%)	9.1 (60.2)
I / σ (I)	11.2 (2.0)
Completeness (%)	98.2 (98.7)
Multiplicity	3.2 (3.1)
CC(1/2)	0.994 (0.626)
Refinement	
Resolution (Å)	31.86 -2.44
No. reflections	14371
R_{work} / R_{free}	0.248 / 0.298
No. atoms	
Protein	3175
N-lobe (residues 519-780)	2239
C-lobe (residues 780-893)	936
Ligand/ion	23
Water	7
Average *B*-factors (Å^2)	
Protein	50.842
N-lobe (residues 519-780)	42.472
C-lobe (residues 780-893)	70.864
Ligand/ion	63.217
Water	35.437
R.m.s. deviations	
Bond lengths (Å)	0.005
Bond angles (°)	1.036
Ramachandran plot (%)	95.4 / 4.3 / 0.3

Materials and methods

Recombinant expression of Nedd4-1 (HECT domain or full length) in *E. coli*

Nedd4-1 in a PGEX6P1 vector plasmid (GST-Nedd4-1) was transformed into BL21 cells (Novagen). 1L TB media containing 100μg/ml ampicillin was inoculated with 50 mL overnight cell culture and incubated at 37°C until OD reached ~3. Then, IPTG (1.0 mM final concentration) was added to the cell culture media at 18°C, followed by 16 hour incubation at the same temperature. Cells were then harvested and lysed by sonication in phosphate buffered saline (PBS) with protease inhibitors (Complete Mini Protease Inhibitor Cocktail, Roche). The supernatant was incubated with glutathione agarose beads (Pierce Biotechnology) for 1 hour at 4°C. The beads were washed three times with PBS and incubated with PreScission Protease (GE Healthcare) for 4h at 23°C to elute Nedd4-1 (elution buffer: 50mM HEPES, 150 mM NaCl, 0.1 mM EDTA 1mM DTT). Mutant plasmids were prepared with Aligent QuickChange kit.

Nedd4-1 HECT sequence:
GPLGSRDYKRKYEFFRRKLKKQNDIPNKFEMKLRRATVLEDSYRRIMGVKRADFLKAR
LWIEFDGEKGLDYGGVAREWFFLISKEMFNPYYGLFEYSATDNYTLQINPNSGLCNEDH
LSYFKFIGRVAGMAVYHGKLLDGFFIRPFYKMMLHKPITLHDMESVDSEYYNSLRWILE
NDPTELDLRFIIDEELFGQTHQHELKNGGSEIVVTNKNKKEYIYLVIQWRFVNRIQKQMA
AFKEGFFELIPQDLIKIFDENELELLMCGLGDVDVNDWREHTKYKNGYSANHQVIQWF
WKAVLMMDSEKRIRLLQFVTGTSRVPMNGFAELYGSNGPQSFTVEQWGTPEKLPRAHT
CFNRLDLPPYESFEELWDKLQMAIENTQGFDGVD

Nedd4-1 full length E554A sequence:
GPLGSMATCAVEVFGLLEDEENSRIVRVRVIAGIGLAKKDILGASDPYVRVTLYDPMNG
VLTSVQTKTIKKSLNPKWNEEILFRVHPQQHRLLFEVFDENRLTRDDFLGQVDVPLYPLP
TENPRLERPYTFKDFVLHPRSHKSRVKGYLRLKMTYLPKTSGSEDDNAEQAEELEPGW
VALDQPDAACHLQQQQEPSPLPPGWEERQDILGRTYYVNHESRRTQWKRPTPQDNLTD
AENGNIQLQAQRAFTTRRQISEETESVDNQESSENWEIIREDEATMYSSQAFPSPPPSSNL
DVPTHLAEELNARLTIFGNSAVSQPASSSNHSSRRGSLQAYTFEEQPTLPVLLPTSSGLPP
GWEEKQDERGRSYYVDHNSRTTTWTKPTVQATVETSQLTSSQSSAGPQSQASTSDSGQ
QVTQPSEIEQGFLPKGWEVRHAPNGRPFFIDHNTKTTTWEDPRLKIPAHLRGKTSLDTSN
DLGPLPPGWEERTHTDGRIFYINHNIKRTQWEDPRLENVAITGPAVPYSRDYKRKYEFFR
RKLKKQNDIPNKFEMKLRRATVLADSYRRIMGVKRADFLKARLWIEFDGEKGLDYGGV
AREWFFLISKEMFNPYYGLFEYSATDNYTLQINPNSGLCNEDHLSYFKFIGRVAGMAVY
HGKLLDGFFIRPFYKMMLHKPITLHDMESVDSEYYNSLRWILENDPTELDLRFIIDEELFG
QTHQHELKNGGSEIVVTNKNKKEYIYLVIQWRFVNRIQKQMAAFKEGFFELIPQDLIKIF
DENELELLMCGLGDVDVNDWREHTKYKNGYSANHQVIQWFWKAVLMMDSEKRIRLL
QFVTGTSRVPMNGFAELYGSNGPQSFTVEQWGTPEKLPRAHTCFNRLDLPPYESFEELW
DKLQMAIENTQGFDGVD

Irreversible Tethering Screening Assay with Nedd4-1 HECT domain

10 μM of Nedd4-1 HECT domain in 50mM HEPES 150mM NaCl 0.1 mM EDTA 1mM DTT pH 7.5 was treated with a mixture of ten fragments (from 10 mM each DMSO stock solution mixtures; final concentrations: 100μM of each fragment, and 1% DMSO). Fragment structures and mixture compositions were the same as reported previously (ref. 14 of the main text). The reaction mixture was incubated for 4h at 23°C before being passed through Zeba gel filtration

columns (Thermo, 7K MWCO) to remove unreacted fragments. The protein solution was then immediately analyzed by whole protein LC/ESI-MS.

LC/ESI-MS Protocol

Accurate-mass data were obtained on an Agilent 6210A LC-TOF mass spectrometer in positive ion mode using electrospray ionization. Samples were chromatographed on the LC-TOF instrument using a Poroshell 120 EC-C18 HPLC column (2.1 * 50 mm, 2.7 micron), an Agilent Series 1200 HPLC binary pump, and an Agilent Series 1200 autoinjector. The HPLC column was held at 45 °C and the autosampler was held at 8 °C. Mobile Phase A was a solution of 0.1% formic acid in water : acetonitrile (19:1). Mobile Phase B was a solution of 0.1 % formic acid in acetonitrile. The flow rate was set to 250 µL/min. The gradient used was 0% B for 2 minutes, ramping linearly to 90% B from 2 minutes to 5 minutes, holding at 90 % B from 5 minutes to 7 minutes, and then returning to 0% B at 7.1 minutes. The column was allowed to equilibrate for 2.7 minutes before the next injection was initiated. The eluent from the column was diverted to waste for the first 2 minutes. The spectra were acquired from 301 to 3200 daltons using a gas temperature of 340 °C, a gas flow of 7 liters/min, and the nebulizer gas at 35 psi. The following voltages were used: capillary 4200 V, fragmentor 230V, skimmer 64V, and octapole RF peak 250V. Spectra were acquired at a rate of 1 spectra/sec. The data was processed using MassHunter software version B.02.00. Maximum entropy deconvolutions were performed with a Mass Step of 1, S/N Threshold of 30, Average Mass at 90% of Peak Height, and 5 Charge States Minimum.

Preparation of fully labeled Nedd4-1•inhibitor complexes for crystallography

10 µM of Nedd4-1 HECT domain in 50mM HEPES 150mM NaCl 0.1 mM EDTA 1mM DTT pH 7.5 was treated with 1mM of inhibitor **1** (from 100 mM DMSO stock solution; final concentrations: 1mM of inhibitor, 1% DMSO, and 0.2% CHAPS to solubilize the inhibitors at 1mM). The reaction mixture was incubated for 4h at 23°C before being passed through Zeba gel filtration columns (Thermo, 7K MWCO) to remove unreacted inhibitor. The protein solution was then immediately used for crystallization or enzymatic assay.

Crystallization

Crystals of the Nedd4 HECT:inhibitor **1** complex were obtained by the sitting-drop vapor diffusion method using MiTeGen - XtalQuest Plates with a 1:1 ratio of protein (6.3mg/mL) and reservoir solution at 20 °C. The precipitant was similar to that used previously[1], and consisted of 100 mM 2-(N-morpholino)ethanesulfonic acid (MES), pH 6.5, 35 mM $CaCl_2$, 5 mM tris(2-carboxyethyl)phosphine (TCEP), 6% polyethylene glycol (PEG) 400. Crystals were soaked in cryoprotectant (100 mM MES, pH 6.0, 6% PEG 400, 20% ethylene glycol) for 1 min, mounted on loops, and flash frozen in $N_{2(l)}$.

Data Collection and Structure Determination

Native data sets were collected using synchrotron radiation at the LS-CAT 21-ID-D beamline at the Advanced Photon Source, Argonne National Laboratory, using a Mar 300 CCD detector. The datasets were processed using Xia2[2] and solved by molecular replacement using Phaser[3]. The coordinates of the Nedd4 HECT structure with Protein Data Bank (PDB) ID 2XBF were used as a starting model. Descriptions of the inhibitor and link were generated with the program JLigand[4] utilizing the appropriate library obtained from the Grade Web Server[5]. Model building

and refinement were performed with Coot[6] and REFMAC5[7,8], respectively. The new chiral center generated upon covalent binding of the inhibitor to the Cys side chain was initially modeled as both *S* and *R* enantiomers. Since the refinement with the *S* enantiomer resulted in a lower R_{work}/R_{free}, we modeled this center as the *S* stereoisomer. However, we note that further experimental evidence is necessary to determine the absolute stereochemistry at this site. Translation liberation screw-rotation (TLS)[7,9] parameters and restrained refinement options in REFMAC5 were used for the final refinement cycles. Ramachandran plots were calculated with PROCHECK[7,10], and validation was performed using both PHENIX[11] and SFCHECK[12]. Data collection and refinement statistics are shown in Table S1. Electron density maps were calculated using FFT[7,13], and figures were prepared using PyMOL[14]. The atomic coordinates have been deposited in the PDB, Research Collaboratory for Structural Bioinformatics at Rutgers University, ID 5C91.

Fluorescence Polarization Assay

Nedd4-1 HECT (8 μM) and ubiquitin-fluorescein (50 nM, Lifesensors) in 50mM HEPES pH 7.5 150mM NaCl 0.1 mM EDTA were treated with DMSO or varying concentrations of inhibitor in 1% DMSO in black 96 well plates. Changes in fluorescence polarization were monitored over 1h with a Biotek Synergy 4 plate reader. Slopes of ln(polarization) vs. time were plotted with GraphPad Prism and used to determine the pseudo-first order rate contstant k_{obs} for a given concentration of inhibitor. The values of k_{inact}/K_I for each inhibitor were then determined by fitting the k_{obs} vs. [inhibitor] plot to the equation $k_{obs}= k_{inact}*[inhibitor]/([inhibitor]+K_I)$. All reactions were performed in triplicate and plotted as mean ±s.e.m.

Preparation of fluorescein-Wbp2-C-K222

Wbp2-C-K222 in a PGEX6P1 vector plasmid (GST-Wbp2-C-K222) was transformed into BL21 cells (Novagen). 1L LB media containing 100μg/ml ampicillin was inoculated with 50 mL overnight cell culture and incubated at 37°C until OD reached ~0.6. Then, IPTG (0.1 mM final concentration) was added to the cell culture media at 18°C, followed by 16 hour incubation at the same temperature. Cells were then harvested and lysed by sonication in phosphate buffered saline (PBS) with protease inhibitors (Complete Mini Protease Inhibitor Cocktail, Roche). The supernatant was incubated with glutathione agarose beads (Pierce Biotechnology) for 1 hour at 4°C. The beads were washed three times with PBS and incubated with PreScission Protease (GE Healthcare) for 16h at 4°C to elute Wbp2-C-K222 (50mM HEPES, 150 mM NaCl, 0.1 mM EDTA 1mM DTT). Wbp2-C-K222 was then treated with 1mM TCEP for 15 min, then 5-iodoacetamidofluorescein (Santa Cruz Biotechnology) in DMSO was added (final concentration: 3mM, 5% DMSO). The reaction was rocked at 4°C for 90 min in the dark, then passed through a Zeba gel filtration column (Thermo, 7K MWCO). The tagged protein was further purified by size exclusion with an S75 column (GE Healthcare). Elution buffer: 20mM Tris-HCl pH 8.0 200mM NaCl 1mM EDTA 5% glycerol 1mM DTT.

***In vitro* ubiquitination assays – Nedd4-1 HECT domain**

Reaction mixtures were composed of 80nM Ube1 E1 enzyme (Boston Biochem), 1.5 μM UbcH5a E2 enzyme (Boston Biochem), 1.5 μM Nedd4-1 HECT domain, 1 μM Flu-Wbp2 substrate, 6 μM ubiquitin (Sigma-Aldrich), and ATP in 25mM HEPES pH 7.6 100mM NaCl 4mM $MgCl_2$. 30 μL reactions were quenched with 6X Laemmli buffer and 3 μL beta-mercaptoethanol and analyzed by SDS-PAGE. Fluorescent gels were imaged with a Typhoon

9400 (GE Healthcare, NCRR #S10RR027842 at Northwestern's Keck Biophysics Facility) and fluorescent bands were quantified with ImageQuant TL. For inhibitor treated assays, Nedd4-1 HECT domain (10μM) was pretreated with inhibitor (100μM in 1% DMSO) for 1h, then used immediately in the enzymatic assay.

***In vitro* ubiquitination assays – Nedd4-1 full length E554A**

Reaction mixtures were composed of 60nM Ube1 E1 enzyme (Boston Biochem), 150 nM UbcH5a E2 enzyme (Boston Biochem), 150 nM Nedd4-1 full length E554A, 100 nM Flu-Wbp2 substrate, 80 μM ubiquitin (Sigma-Aldrich), and ATP in 25mM HEPES pH 7.6 100mM NaCl 4mM $MgCl_2$. 30 μL reactions were quenched with 6X Laemmli buffer and 3 μL beta-mercaptoethanol and analyzed by SDS-PAGE. Fluorescent gels were imaged with a Typhoon 9400 (GE Healthcare, NCRR #S10RR027842 at Northwestern's Keck Biophysics Facility) and fluorescent bands were quantified with ImageQuant TL. For inhibitor treated assays, Nedd4-1 full length E554A (10μM) was pretreated with inhibitor (100μM in 1% DMSO) for 1h, then diluted to 1μM and used immediately in the enzymatic assay.

Recombinant expression of USP08 catalytic domain in *E. coli*

USP08 catalytic domain in a PET21a-LIC vector plasmid (6×His-USP08, Addgene) was transformed into BL21 (DE3) cells (Invitrogen). 1L TB media containing 100μM kanamycin and 600μl antifoam 204 (Sigma A-8311) was inoculated with 50ml overnight culture and incubated at 37°C until OD reached ~3. Then, IPTG (100 μM final concentration) was added to the cell culture media at 15°C. The culture was incubated overnight at the same temperature. Cells were then harvested and lysed by sonication in 10 mM Tris-HCl pH 7.0, 0.5 M NaCl 5% glycerol 2 mM imidazole 1 mM β-mercaptoethanol 0.1 μM PMSF. The cleared lysate was then loaded onto TALON metal-affinity beads at 4°C. Beads were washed three times with 10 mM Tris-HCl, pH 7.0 0.5 M NaCl 5% glycerol 10 mM imidazole 1 mM β-mercaptoethanol 0.05% Tween 20. The protein was then eluted with 10 mM Tris-HCl pH 7.0, 0.5 M NaCl 5% glycerol 200 mM imidazole 1 mM β-mercaptoethanol before being exchanged into 50mM HEPES 150mM NaCl 0.1mM EDTA pH 7.5 with PD10 columns (GE Healthcare). MS analysis of USP08 showed that the resulting protein had a cleaved N-terminal methionine residue, and ~50% of the protein had been further modified by gluconic acid at the N-terminus.

Chemical Synthesis

General Information

Methanol (ACS grade), ethyl acetate (ACS grade), chloroform (ACS grade), toluene (ACS grade), and diethyl ether (ACS grade), acetonitrile (HPLC grade), and hexanes (ACS grade) were purchased from Fisher Scientific and used without further purification. Dichloromethane, tetrahydrofuran and dimethylformamide were purified by passing over activated alumina. Commercially available reagents were used without further purification. Unless otherwise specified, all reagents were purchased from Sigma-Aldrich. Reactions were monitored by thin-layer chromatography (TLC) on pre-coated glass backed plates (60 Å silica gel, 0.25mm, Whatman), and components were visualized by UV light (254 and 365 nm) or by treating the plates with anisaldehyde, $KMnO_4$, and ninhydrin stains followed by heating. Flash column chromatography was performed over ultra pure silica gel (230-400 mesh) from Silicycle. ^1H and ^{13}C NMR spectra were obtained on a Bruker AVANCE III 500 MHz spectrometer or an Agilent DDR2 400 MHz spectrometer (Funded by NSF CHE-1048773, 2010) at Northwestern's Integrated Molecular Structure Education and Research Center. Chemical shifts were reported in ppm relative to the residual solvent peak ($CDCl_3$ or DMSO-d_6). Multiplicity was indicated as follows: s (singlet); d (doublet); t (triplet); q (quartet); m (multiplet); dd (doublet of doublets); ddd (doublet of doublet of doublets); dt (doublets of triplets); td (triplet of doublets). Coupling constants were reported in Hz. Small molecule ESI-MS was performed on a Bruker AmaZon SL quadropole ion trap instrument.

General Synthesis Scheme

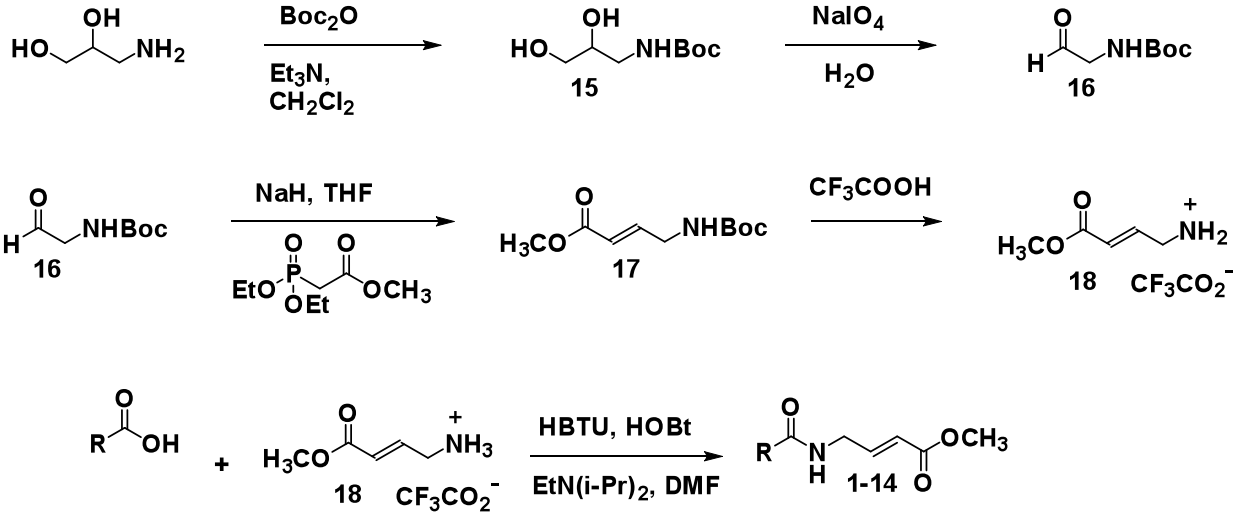

Synthesis of 15

(±)-3-amino-1,2-propanediol (11.29 g, 124 mmol) was dissolved in CH_2Cl_2:CH_3OH (1:5) (1M) and triethylamine (2 mL, 14.7 mmol) was added. Di-tert-butyl dicarbonate (32.5g, 149 mmol) was dissolved in dichloromethane (0.8M, 186 mL) and added slowly to the reaction mixture. The resulting reaction was stirred at 23°C for 2h, followed by TLC analysis that showed a full consumption of the starting material. The reaction mixture was evaporated under reduced pressure, and the residue was purified by column chromatography with EtOAc:Hexanes 1:4, then dried on high vacuum to yield **15** as a white solid (23.7g, 94% yield). ^1H NMR (500 MHz, $CDCl_3$) δ 5.28 – 4.96 (m, 1H), 3.83 – 3.73 (m, 1H), 3.60 (qd, J = 11.7, 4.9 Hz, 2H), 3.44 (s, 1H),

3.27 (dt, J = 12.9, 6.0 Hz, 2H), 1.46 (s, 9H). ^{13}C NMR (126 MHz, Chloroform-d) δ 157.45 , 80.13 , 71.37 , 63.58 , 28.35 , 27.42.

Synthesis of 16

15 (10 g, 52mmol) was suspended in H_2O (0.6M, 87.2mL) and the flask was covered in foil (to protect $NaIO_4$ from light). $NaIO_4$ (13.4g, 62.8 mmol) was then added and the reaction was stirred for 1h. A white precipitate had formed after 1h, and TLC analysis showed full consuption of the starting material. The precipitate was filtered off, and the aqueous layer was extracted with $CHCl_3$ (8×50 mL). The organic layer was dried with $MgSO_4$, filtered, and evaporated to yield **16** as a yellow oil, which was used immediately without further purification (7.7g, 93% yield). ^{1}H NMR (500 MHz, $CDCl_3$) δ 9.68 (s, 1H), 5.23 (s, 1H), 4.10 (d, J = 5.2 Hz, 2H), 1.47 (s, 9H). ^{13}C NMR (126 MHz, $CDCl_3$) δ 197.21 , 155.67 , 80.19 , 51.39, 28.28.

Synthesis of 17

Sodium hydride (60% dispersion in mineral oil) (1.9 g, 46.6 mmol) in tetrahydrofuran (0.17 M, 274 mL) was cooled to 0°C, then triethylphosphonoacetate (8.5 mL, 46.6 mmol) in THF was added dropwise. The reaction was stirred at 0°C for 20 min, then **16** (7.4 g, 46.6 mmol) in THF was added. The reaction was allowed to warm to 23°C and was stirred for 1h. TLC showed a full consuption of the starting materials and conversion to product. THF was removed under reduced pressure, and the residue was then diluted with ethyl acetate (200mL) and water (200 mL). The layers were separated, followed by the extraction of the aqueous layer with EtOAc (2×100 mL). The organic layer was then dried over $MgSO_4$, filtered, and evaporated. The residue was purified by flash column chromatography with an ethyl acetate/hexanes gradient 25% EtOAc → 50% EtOAc to yield **17** (6.6g, 66% yield). ^{1}H NMR (500 MHz, $CDCl_3$) δ 6.94 (dt, J = 15.7, 4.8 Hz, 1H), 5.97 (dt, J = 15.8, 1.9 Hz, 1H), 4.73 (s, 1H), 3.95 (t, J = 5.6 Hz, 2H), 3.76 (s, 3H), 1.48 (s, 9H). ^{13}C NMR (126 MHz, $CDCl_3$) δ 166.55 , 145.26 , 120.71 , 79.73 , 60.37 , 51.58 , 41.28 , 28.30.

Synthesis of 18

17 (6.6 g, 30.8 mmol) was dissolved in trifluoroacetic acid (47 mL, 617 mmol) and stirred at 23°C for 30 min. TLC at 30 min showed conversion to product. TFA was evaporated and azeotroped with toluene (2×100mL). The residue was then dried on high vacuum for 2 hours, dissolved in 2 mL methanol and dropped into ice cold diethyl ether (200 mL). The ether was then filtered to collect **18** as the TFA salt (6.2 g, 88% yield). ^{1}H NMR (500 MHz, DMSO-d_6) δ 8.08 (s, 3H), 6.86 (dt, J = 15.9, 5.6 Hz, 1H), 6.15 (dt, J = 16.0, 1.7 Hz, 1H), 3.70 (s, 3H), 3.70 (d, J = 1.8 Hz, 2H). ^{13}C NMR (126 MHz, DMSO-d_6) δ 165.33 , 140.61 , 123.22 , 51.72 .

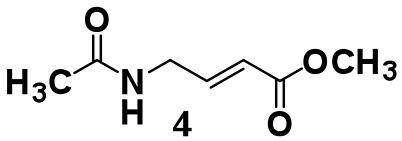

Synthesis of 4 (methyl (E)-4-acetamidobut-2-enoate) 18, TFA (50mg, 0.218 mmol) and triethylamine (77.8μL, 0.558 mmol) were dissolved in anhydrous CH_2Cl_2 (2.4 mL, 0.09M), then acetic anhydride (32.1μL, 0.34 mmol) was added dropwise. The reaction was stirred at 23°C for 24h, at which point TLC showed conversion to product. The reaction was quenched with 10mL saturated NH_4Cl, then extracted with 10% CH_3OH/CH_2Cl_2 (3x10mL). The combined organic

layers were dried over $MgSO_4$, filtered, and evaporated. Purification with flash column chromatography with CH_3OH/CH_2Cl_2 (CH_3OH gradient 0→5%) yielded compound **4** (23.3 mg, 68% yield). ^1H NMR (500 MHz, $CDCl_3$) δ 6.93 (dt, J = 15.7, 5.1 Hz, 1H), 5.95 (dt, J = 15.8, 1.8 Hz, 1H), 5.68 (s, 1H), 4.08 (td, J = 5.8, 1.8 Hz, 2H), 3.76 (s, 3H), 2.07 (s, 3H). ^{13}C NMR (126 MHz, $CDCl_3$) δ 169.98, 166.39, 144.13, 121.48, 51.70, 40.21, 23.14. [M+Na]: 179.828 Da.

Synthesis of 1, 2, 3, 5-14

The commercially available carboxylic acid starting material (0.35 mmol) was dissolved in dimethylformamide (0.2M, 1.75 mL), then **18**, TFA (80.2 mg, 0.35 mmol), HBTU (128mg, 0.34 mmol), and HOBT (51.8 mg, 0.38 mmol) were added, followed by diisopropylethylamine (175 μL, 1.047 mmol). The reaction was stirred at 23°C for 16h. TLC at 16h showed conversion to product. The reaction was quenched with H_2O (5mL) and extracted with DCM (3×5mL). The combined organic layers were washed with 1M HCl (10mL), saturated aqueous $NaHCO_3$ (10mL), and saturated aqueous NaCl (10mL). The organic layer was dried over $MgSO_4$, filtered, and evaporated. Purification with flash column chromatography with CH_3OH/CH_2Cl_2 (CH_3OH gradient 0→5%) yielded compounds **1, 2, 3, 5-14.**

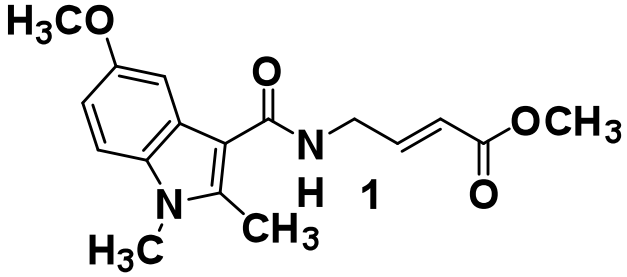

Methyl(E)-4-(5-methoxy-1,2-dimethyl-1H-indole-3-carboxamido)but-2-enoate (compound 1) Carboxylic acid starting material purchased from ChemBridge. 55.6 mg, 50.2% yield. ^1H NMR (500 MHz, $CDCl_3$) δ 7.28 – 7.21 (m, 2H), 7.11 (dt, J = 15.7, 4.9 Hz, 1H), 6.91 (dd, J = 8.8, 2.4 Hz, 1H), 4.34 (ddd, J = 6.1, 4.9, 2.0 Hz, 2H), 3.91 (s, 3H), 3.76 (s, 3H), 3.70 (s, 3H), 2.74 (s, 3H). ^{13}C NMR (126 MHz, $CDCl_3$) δ 166.57, 166.28, 155.32, 145.26, 142.70, 131.76, 125.59, 121.15, 110.59, 110.30, 106.82, 101.91, 56.05, 51.67, 40.16, 29.68, 11.84. [M+Na]: 339.244 Da.

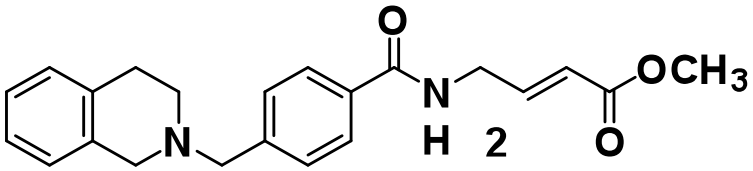

Methyl(E)-4-(4-((3,4-dihydroisoquinolin-2(1H)-yl)methyl)benzamido)but-2-enoate (compound 2) Carboxylic acid starting material purchased from ChemBridge. 103.22 mg, 80.7% yield. ^1H NMR (500 MHz, DMSO-d_6) δ 8.82 (t, J = 5.7 Hz, 1H), 7.87 (d, J = 8.2 Hz, 2H), 7.47 (d, J = 8.2 Hz, 2H), 7.18 – 7.04 (m, 3H), 7.04 – 6.86 (m, 2H), 5.92 (dt, J = 15.7, 1.9 Hz, 1H), 4.23 – 3.99 (m, 2H), 3.71 (s, 2H), 3.66 (s, 3H), 3.55 (s, 2H), 2.82 (d, J = 5.8 Hz, 2H), 2.69 (s, 3H). ^{13}C NMR (126 MHz, DMSO-d_6) δ 166.08, 165.89, 146.28, 142.08, 134.66, 134.00, 132.69, 128.51, 128.42, 127.26, 126.32, 125.97, 125.45, 119.93, 61.35, 55.40, 51.37, 50.25, 38.21, 28.64. [M+H]: 363.255 Da.

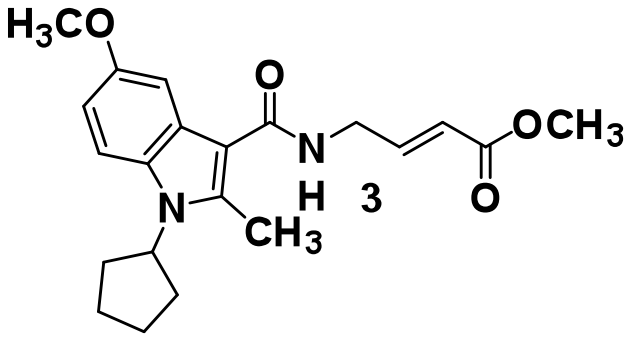

Methyl(E)-4-(1-cyclopentyl-5-methoxy-2-methyl-1H-indole-3-carboxamido)but-2-enoate (compound 3) Carboxylic acid starting material purchased from Enamine. 78.8 mg, 60.8%. ^{1}H NMR (500 MHz, $CDCl_3$) δ 7.33 (d, J = 8.9 Hz, 1H), 7.24 (d, J = 2.4 Hz, 1H), 7.08 (dt, J = 15.7, 4.9 Hz, 1H), 6.83 (dd, J = 8.9, 2.4 Hz, 1H), 6.05 (dt, J = 15.6, 1.7 Hz, 1H), 6.01 – 5.90 (m, 1H), 4.82 (t, J = 9.0 Hz, 1H), 4.31 (td, J = 5.6, 1.8 Hz, 2H), 3.87 (s, 3H), 3.74 (s, 3H), 2.72 (s, 3H), 2.24 (td, J = 8.6, 5.3 Hz, 2H), 2.06 (dt, J = 10.7, 7.2 Hz, 5H), 1.81 (q, J = 6.5 Hz, 2H). ^{13}C NMR (126 MHz, $CDCl_3$) δ 166.53, 154.88, 145.17, 142.29, 129.10, 126.85, 121.19, 112.42, 110.16, 107.19, 102.08, 56.00, 55.96, 51.63, 40.21, 29.99, 25.38, 12.28. [M+Na]: 392.971 Da.

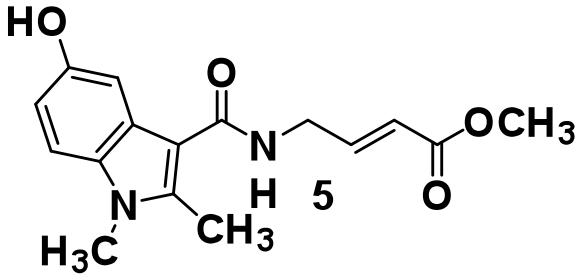

Methyl(E)-4-(5-hydroxy-1,2-dimethyl-1H-indole-3-carboxamido)but-2-enoate (compound 5) Carboxylic acid starting material purchased from Chembridge. 26.2 mg, 24.7% yield. ^{1}H NMR (400 MHz, $CDCl_3$) δ 7.19 – 7.10 (m, 2H), 7.04 (dt, J = 15.7, 5.1 Hz, 1H), 6.78 (dd, J = 8.7, 2.4 Hz, 1H), 6.01 (dt, J = 15.6, 1.9 Hz, 1H), 4.27 (td, J = 5.5, 1.9 Hz, 2H), 3.72 (s, 3H), 3.64 (s, 3H), 2.68 (s, 3H).

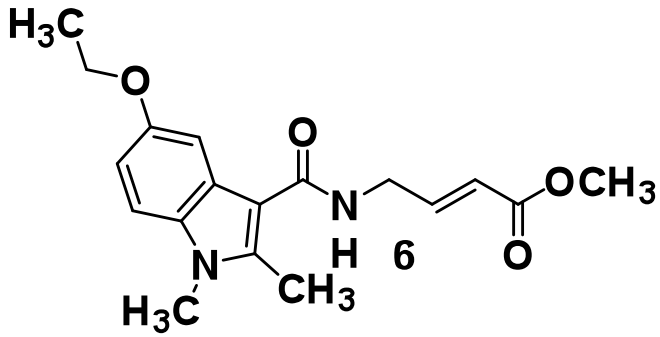

Methyl(E)-4-(5-ethoxy-1,2-dimethyl-1H-indole-3-carboxamido)but-2-enoate (compound 6) Carboxylic acid starting material purchased from Chembridge. 48.3 mg, 41.6% yield. ^{1}H NMR (400 MHz, $CDCl_3$) δ 7.23 – 7.16 (m, 2H), 7.06 (dt, J = 15.7, 5.0 Hz, 1H), 6.91 – 6.79 (m, 1H), 6.02 (d, J = 15.7 Hz, 1H), 5.99 – 5.91 (m, 1H), 4.28 (ddd, J = 5.9, 5.0, 1.9 Hz, 2H), 4.08 (q, J = 7.0 Hz, 2H), 3.72 (s, 3H), 3.65 (s, 3H), 2.69 (s, 3H), 1.43 (t, J = 7.0 Hz, 3H). ^{13}C NMR (126

MHz, $CDCl_3$) δ 166.56, 166.27, 154.61, 145.27, 142.83, 131.80, 125.59, 121.15, 111.08, 110.22, 106.76, 103.03, 64.42, 51.62, 40.16, 29.62, 15.06, 11.79. [M+Na]: 352.952 Da.

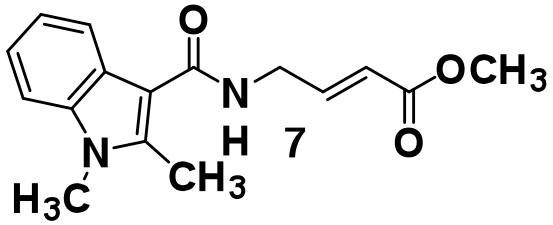

Methyl(E)-4-(1,2-dimethyl-1H-indole-3-carboxamido)but-2-enoate (compound 7) Carboxylic acid starting material purchased from Chembridge. 71.05 mg, 70.7% yield. ^{1}H NMR (400 MHz, $CDCl_3$) δ 7.75 – 7.58 (m, 1H), 7.41 – 7.28 (m, 1H), 7.27 – 7.15 (m, 3H), 7.06 (dt, J = 15.7, 5.0 Hz, 1H), 6.08 (s, 1H), 6.02 (dt, J = 15.7, 1.9 Hz, 1H), 4.30 (ddd, J = 5.9, 5.0, 1.9 Hz, 2H), 3.72 (s, 3H), 3.69 (s, 3H), 2.73 (s, 3H). ^{13}C NMR (126 MHz, $CDCl_3$) δ 166.58, 166.17, 145.14, 142.87, 136.52, 124.83, 121.31, 118.31, 109.73, 106.97, 51.64, 40.18, 29.53, 11.67. [M+Na]: 308.858 Da.

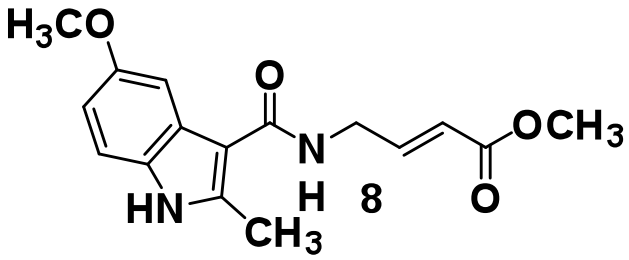

Methyl(E)-4-(5-methoxy-2-methyl-1H-indole-3-carboxamido)but-2-enoate (compound 8) Carboxylic acid starting material purchased from Matrix Scientific. 43.3 mg, 40.88%. ^{1}H NMR (400 MHz, $CDCl_3$) δ 7.23 – 7.17 (m, 2H), 7.05 (dt, J = 15.7, 5.0 Hz, 1H), 6.82 (dd, J = 8.7, 2.4 Hz, 1H), 6.03 (d, J = 15.7 Hz, 0H), 5.96 (t, J = 6.1 Hz, 1H), 4.29 (ddd, J = 6.0, 5.0, 1.9 Hz, 2H), 3.85 (s, 3H), 3.72 (s, 3H), 2.68 (s, 3H).

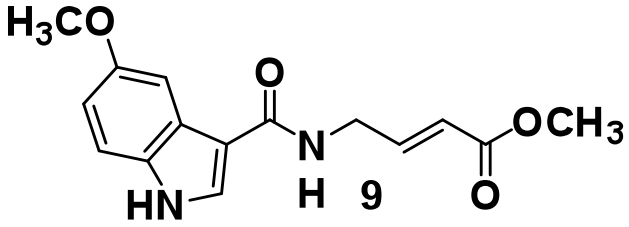

Methyl(E)-4-(5-methoxy-1H-indole-3-carboxamido)but-2-enoate (compound 9) Carboxylic acid starting material purchased from Sigma-Aldrich. 17.1 mg, 16.9% yield. ^{1}H NMR (400 MHz, $CDCl_3$) δ 8.36 (s, 1H), 7.66 (d, J = 3.0 Hz, 1H), 7.55 (d, J = 2.5 Hz, 1H), 7.30 (dd, J = 8.9, 0.6 Hz, 1H), 7.04 (dt, J = 15.7, 5.0 Hz, 1H), 6.92 (dd, J = 8.9, 2.4 Hz, 1H), 6.03 (d, J = 15.7 Hz, 1H), 5.97 (s, 1H), 4.28 (ddd, J = 6.0, 5.0, 1.9 Hz, 2H), 3.88 (s, 3H), 3.72 (s, 3H). ^{13}C NMR (126 MHz, $CDCl_3$) δ 166.93, 166.00, 155.39, 145.31, 131.49, 131.34, 128.13, 127.96, 125.89, 125.86, 113.09, 112.62, 112.57, 110.68, 110.63, 102.23, 55.85, 51.68, 39.96. [M+Na]: 310.842 Da.

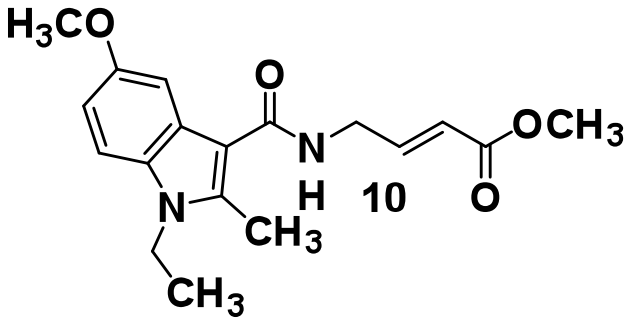

Methyl(E)-4-(1-ethyl-5-methoxy-2-methyl-1H-indole-3-carboxamido)but-2-enoate (compound 10) Carboxylic acid starting material purchased from Enamine. 68.95 mg, 59.4% yield. ^{1}H NMR (400 MHz, $CDCl_3$) δ 7.22 (d, J = 10.8 Hz, 1H), 7.06 (dt, J = 15.7, 5.0 Hz, 1H), 6.86 (dd, J = 8.8, 2.4 Hz, 1H), 6.03 (d, J = 15.7 Hz, 1H), 5.96 (t, J = 5.9 Hz, 1H), 4.29 (ddd, J = 5.9, 5.0, 1.9 Hz, 2H), 4.11 (t, J = 7.2 Hz, 2H), 3.86 (s, 3H), 3.71 (s, 3H), 2.69 (s, 3H), 1.33 (t, J = 7.2 Hz, 3H). ^{13}C NMR (126 MHz, $CDCl_3$) δ 166.50, 155.36, 144.97, 142.00, 130.63, 125.84, 121.32, 110.71, 110.37, 102.00, 56.06, 51.65, 40.27, 37.98, 29.73, 14.94, 11.59. [M+Na]: 352.918 Da.

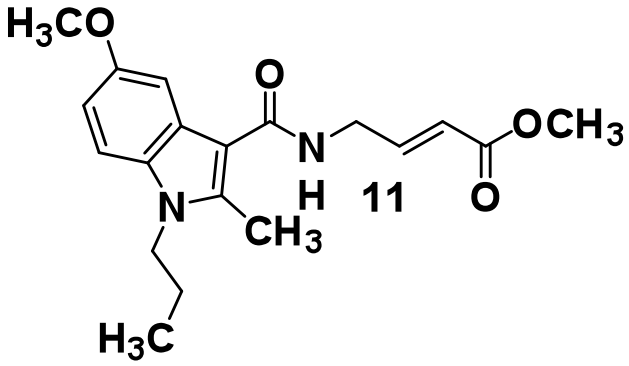

Methyl(E)-4-(5-methoxy-2-methyl-1-propyl-1H-indole-3-carboxamido)but-2-enoate (Compound 11) Carboxylic acid starting material purchased from Enamine. 57.4 mg, 47.6% yield. ^{1}H NMR (500 MHz, $CDCl_3$) δ 7.24 (d, J = 1.5 Hz, 1H), 7.10 (dt, J = 15.7, 4.9 Hz, 1H), 6.89 (dd, J = 8.8, 2.4 Hz, 1H), 6.07 (d, J = 15.7 Hz, 1H), 6.03 (dd, J = 12.2, 5.7 Hz, 1H), 4.33 (ddd, J = 6.0, 4.9, 1.9 Hz, 2H), 4.06 (t, J = 7.4 Hz, 2H), 3.89 (s, 3H), 3.75 (s, 3H), 2.72 (s, 3H), 1.81 (q, J = 7.4 Hz, 2H), 0.98 (t, J = 7.4 Hz, 3H). ^{13}C NMR (126 MHz, $CDCl_3$) δ 166.54, 166.34, 155.26, 145.23, 142.21, 131.15, 125.77, 121.19, 110.62, 110.57, 106.90, 101.93, 56.05, 51.63, 44.83, 40.17, 23.16, 11.80, 11.44. [M+Na]: 366.934 Da.

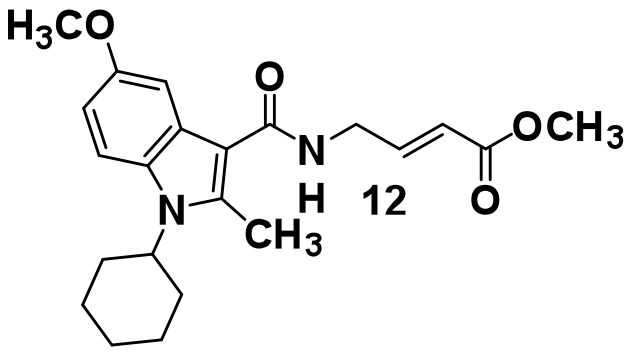

Methyl(E)-4-(1-cyclohexyl-5-methoxy-2-methyl-1H-indole-3-carboxamido)but-2-enoate (compound 12) Carboxylic acid starting material purchased from Enamine. 63.5 mg, 47.2% yield ^{1}H NMR (500 MHz, $CDCl_3$) δ 7.50 (d, J = 9.1 Hz, 1H), 7.24 (d, J = 2.5 Hz, 1H), 7.14 – 7.03 (m, 1H), 6.85 (dd, J = 9.0, 2.5 Hz, 1H), 6.07 (d, J = 15.7 Hz, 1H), 6.02 (d, J = 7.0 Hz, 1H), 4.33 (ddd, J = 5.9, 4.9, 2.0 Hz, 2H), 4.24 (tt, J = 12.3, 4.1 Hz, 1H), 3.89 (s, 3H), 3.76 (s, 3H), 2.74 (s, 3H), 2.43 – 2.19 (m, 2H), 2.00 (dt, J = 14.0, 3.3 Hz, 2H), 1.87 (ddd, J = 24.5, 12.7, 4.0 Hz, 4H), 1.57 – 1.43 (m, 2H). ^{13}C NMR (126 MHz, $CDCl_3$) δ 166.53, 154.73, 145.16, 141.62, 121.19, 110.19, 101.74, 55.95, 51.63, 40.22, 31.25, 26.37, 25.47. [M+Na]: 406.993 Da.

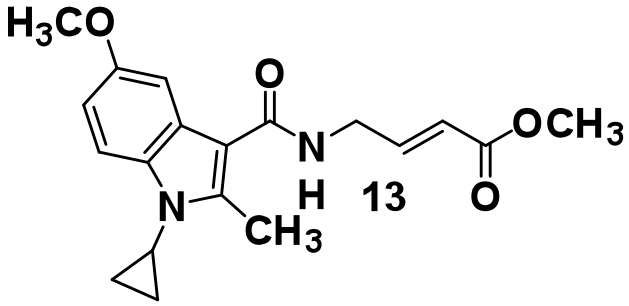

Methyl(E)-4-(1-cyclopropyl-5-methoxy-2-methyl-1H-indole-3-carboxamido)but-2-enoate (compound 13) Carboxylic acid starting material purchased from Enamine. 71.2 mg, 59.4% yield. ^{1}H NMR (500 MHz, $CDCl_3$) δ 7.51 (d, J = 8.9 Hz, 1H), 7.24 (d, J = 2.2 Hz, 1H), 7.09 (ddd, J = 15.7, 5.8, 4.7 Hz, 1H), 6.89 (ddd, J = 9.2, 2.3, 1.1 Hz, 1H), 6.06 (dd, J = 16.0, 1.9 Hz, 1H), 6.02 (d, J = 7.0 Hz, 1H), 4.32 (td, J = 5.4, 4.7, 1.6 Hz, 2H), 3.89 (d, J = 1.1 Hz, 3H), 3.76 (d, J = 1.2 Hz, 3H), 3.15 (dt, J = 7.0, 3.1 Hz, 1H), 2.79 (d, J = 1.2 Hz, 3H), 1.25 (dt, J = 6.9, 1.6 Hz, 2H), 1.15 – 0.96 (m, 2H). ^{13}C NMR (126 MHz, $CDCl_3$) δ 166.51, 155.35, 145.09, 144.42, 132.36, 125.68, 121.23, 111.81, 110.62, 56.03, 51.64, 40.18, 24.95, 12.96, 7.54. [M+Na]: 364.920 Da.

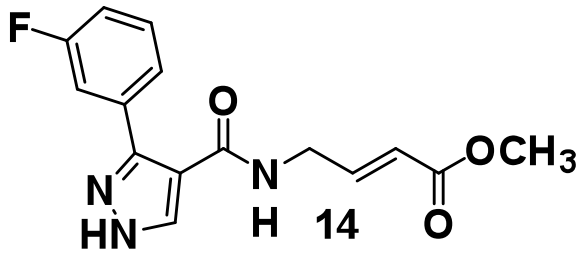

Methyl(E)-4-(3-(3-fluorophenyl)-1H-pyrazole-4-carboxamido)but-2-enoate (compound 14) Carboxylic acid starting material purchased from ChemBridge. 56.9 mg, 53.4% yield. ^{1}H NMR (500 MHz, $CDCl_3$) δ 8.11 (s, 1H), 7.55 – 7.43 (m, 2H), 7.41 (ddd, J = 9.5, 2.6, 1.5 Hz, 1H), 7.20 (tdd, J = 8.4, 2.7, 1.2 Hz, 1H), 6.92 (dt, J = 15.7, 5.1 Hz, 1H), 5.85 (dt, J = 15.7, 1.9 Hz, 1H), 5.79 (t, J = 6.0 Hz, 1H), 4.15 (ddd, J = 6.1, 5.2, 1.9 Hz, 2H), 3.76 (s, 3H). ^{13}C NMR (126 MHz, $CDCl_3$) δ 166.46, 163.73, 163.16, 161.77, 143.89, 130.58, 130.52, 124.66, 124.63, 121.45, 116.47, 116.30, 116.10, 115.92, 115.09, 55.59, 51.73, 43.53, 40.18, 18.56, 17.21, 12.42. [M+Na]: 325.846 Da.

Supplementary references

[1] Maspero, E.; Mari, S.; Valentini, E.; Musacchio, A.; Fish, A.; Pasqualato, S.; Polo, S. Structure of the HECT:ubiquitin complex and its role in ubiquitin chain elongation. *EMBO Rep*. **2011**, *12*, 342.

[2] Winter, G. Xia2: an expert system for macromolecular crystallography data reduction. *J. Appl. Cryst.* **2010**, *43*, 186.

[3] McCoy, A.J.; Grosse-Kunstleve, R.W.; Adams, P. D.; Winn, M. D.; Storoni, L. C.; Read, R. J. Phaser crystallographic software. *J. Appl. Cryst.* **2007**, *40*, 658.

[4] Lebedev, A. A.; Young, P.; Isupov, M. N.; Moroz, O. V.; Vagin, A. A.; Murshudov, G. N. JLigand: a graphical tool for the CCP4 template-restraint library. *Acta Cryst. D* **2012**, *68*.

[5] Smart, O. S.; Womack, T. O.; Sharff, A.; Flensburg, C.; Keller, P.; Paciorek, W.; Vonrhein, C.; Bricogne, G. (2011) grade, version 1.101. Cambridge, United Kingdom, Global Phasing Ltd., http://www.globalphasing.com

[6] Emsley, P.; Cowtan, K. Coot: model-building tools for molecular graphics. *Acta Cryst. D* **2004**, *60*, 2126.

[7] Winn, M. D.; Ballard, C. C.; Cowtan, K. D.; Dodson, E. J.; Emsley, P.; Evans, P. R.; Keegan, R. M.; Krissinel, E. B.; Leslie, A. G. W.; McCoy, A.; McNicholas, S. J.; Murshudov, G. N.; Pannu, N. S.; Potterton, E. A.; Powell, H. R.; Read, R. J.; Vagin, A.; Wilson, K. S. Overview of the CCP4 suite and current developments. *Acta Cryst. D* **2011**, *67*, 235.

[8] Murshudov, G. N.; Vagin, A. A.; Dodson, E. J. Refinement of macromolecular structures by the maximum-likelihood method. *Acta Cryst. D* **1997**, *53*, 240.

[9] Winn, M. D.; Isupov, M. N.; Murshudov, G. N. Use of TLS parameters to model anisotropic displacements in macromolecular refinement. *Acta Cryst. D* **2001**, *57*, 122.

[10] Laskowski, R. A.; Rullmannn, J. A.; MacArthur, M. W.; Kaptein, R.; Thornton, J. M. J. AQUA and PROCHECK-NMR: programs for checking the quality of protein structures solved by NMR. *Biomol. NMR* **1996**, *8*, 477.

[11] Adams, P. D.; Afonine, P. V.; Bunkoczi, G.; Chen, V. B.; Davis, I. W.; Echols, N.; Headd, J. J.; Hung, L.-W.; Kapral, G. J.; Grosse-Kunstleve, R. W.; McCoy, A. J.; Moriarty, N. W.; Oeffner, R.; Read, R. J.; Richardson, D. C.; Richardson, J. S.; Terwilliger, T. C.; Zwart, P. H. *Acta Cryst. D* **2010**, *66*, 213.

[12] Vaguine, A. A.; Richelle, J.; Wodak, S. J. SFCHECK: a unified set of procedures for evaluating the quality of macromolecular structure-factor data and their agreement with the atomic model. *Acta Cryst. D* **1999**, *55*, 191.

[13] Read, R. J.; Schierbeek, A. J. J. A phased translation function. *J. Appl. Cryst.* **1988**, *21*, 490.

[14] The PyMOL Molecular Graphics System, Version 1.3; Schrödinger, LLC.